

animal2vec and MeerKAT

A self-supervised transformer for rare-event raw audio input and a large-scale reference dataset for bioacoustics

Julian C. Schäfer-Zimmermann,^{1,2,3,*} Vlad Demartsev,^{1,2,3,4} Baptiste Averly,^{1,2,3,4} Kiran Dhanjal-Adams,^{1,2,3} Mathieu Duteil,^{1,2,3} Gabriella Gall,^{1,2,3,5} Marius Faiß,^{1,2} Lily Johnson-Ulrich,^{4,6} Dan Stowell,^{7,8} Marta B. Manser,^{4,6,9} Marie A. Roch,^{10,†} and Ariana Strandburg-Peshkin^{1,2,3,4,†}

¹Department for the Ecology of Animal Societies, Max Planck Institute of Animal Behavior, Konstanz, Germany

²Department of Biology, University of Konstanz, Konstanz, Germany

³Centre for the Advanced Study of Collective Behaviour, University of Konstanz, Konstanz, Germany

⁴Kalahari Research Centre, Van Zylsrus, Northern Cape, South Africa

⁵Zukunftskolleg, University of Konstanz, Konstanz, Germany

⁶Department of Evolutionary Biology and Environmental Studies, University of Zurich, Zurich, Switzerland

⁷Department of Cognitive Science and Artificial Intelligence, Tilburg University, Tilburg, The Netherlands

⁸Naturalis Biodiversity Center, Leiden, The Netherlands

⁹Interdisciplinary Center for the Evolution of Language, University of Zurich, Zurich, Switzerland

¹⁰Department of Computer Science, San Diego State University, San Diego, California, USA

(Dated: June 4, 2024)

Bioacoustic research provides invaluable insights into the behavior, ecology, and conservation of animals. Most bioacoustic datasets consist of long recordings where events of interest, such as vocalizations, are exceedingly rare. Analyzing these datasets poses a monumental challenge to researchers, where deep learning techniques have emerged as a standard method. Their adaptation remains challenging, focusing on models conceived for computer vision, where the audio waveforms are engineered into spectrographic representations for training and inference. We improve the current state of deep learning in bioacoustics in two ways: First, we present the *animal2vec* framework: a fully interpretable transformer model and self-supervised training scheme tailored for sparse and unbalanced bioacoustic data. *animal2vec* learns general representations from audio waveforms without labels and then uses a second training step to finetune the representations based on labeled data. Second, we openly publish *MeerKAT: Meerkat Kalahari Audio Transcripts*, a large-scale dataset containing audio collected via biologists deployed on free-ranging meerkats with a length of over 1068 h, of which 184 h have twelve time-resolved vocalization-type ground truth target classes, each with millisecond-resolution, making it the largest publicly-available labeled dataset on non-human terrestrial mammals to date. Further, we benchmark *animal2vec* against the publicly available *NIPS4Bplus* birdsong dataset. We report new state-of-the-art classification performance on both datasets and evaluate the few-shot capabilities of *animal2vec* of labeled training data. Finally, we perform ablation studies to highlight the differences between our architecture and a vanilla transformer baseline for human-produced sounds. *animal2vec* allows researchers to classify massive amounts of sparse bioacoustic data even with little ground truth information available. In addition, the *MeerKAT* dataset is the first large-scale, millisecond-resolution corpus for benchmarking bioacoustic models in the pretrain/finetune paradigm. We believe this sets the stage for a new reference point for bioacoustics.

Keywords: self-supervised deep learning; bioacoustics; animal vocalizations; transformer; reference dataset

1. Introduction

Bioacoustics, the study of animal sounds, reveals invaluable insights into the behavior [1, 2], ecology [3, 4], and conservation [5, 6] of animal species. Automated analysis of acoustic recordings can greatly advance the types of questions that can be asked by enabling annotation of long-duration recordings covering multiple seasons and years. While existing datasets cover extensive hours, events of interest such as vocalizations are often sparse, brief, and in noisy conditions, making manual analysis challenging [7–14].

Generally, deep learning is a common approach to tackle large and dense datasets [15], where, recently, transformer-based models [16] have achieved state-of-the-art results across many tasks and modalities [17]. However, there is a lack of such large-scale datasets and training approaches for sparse data using next-generation transformer-based models within bioacoustics [18]. To fill this gap, we introduce the *animal2vec* framework and the *MeerKAT* dataset. *animal2vec* is an interpretable transformer model and training scheme tailored for sparse and unbalanced bioacoustic data, achieving state-of-the-art results, and *MeerKAT: Meerkat Kalahari Audio Transcripts*, is the largest publicly-available labeled dataset on non-human terrestrial mammals to date.

* jzimmermann@ab.mpg.de

† Shared senior authorship

Currently, in bioacoustics, the primary data (audio waveforms) are usually feature-engineered into spectrograms for input to convolutional neural network models (CNNs) originally designed for computer vision [18]. However, using spectrograms and CNNs is justified more by empirical success than conceptual fitness. Spectrograms challenge the notion of translational invariance in CNNs [19], discard phase information or temporal fine structure [18], and the commonly used Mel-scale biases the input toward human hearing [18]. Further, in computer vision, attention-based encoder-only Visual transformers (ViTs) [20, 21] have replaced CNNs, excelling through large-scale pretraining on dense datasets. In this context, pretraining is a method of learning a general model, which can then be finetuned on downstream tasks. This training paradigm is referred to as pretraining/finetune. Current best-performing pretraining strategies include either supervised [20] or contrastive learning (CLR) [22–24]. Pretraining in CLR enforces to pull similar data points (different patches of the same image) together and pushing dissimilar ones (patches from other images in the batch) apart in a latent representation space [24].

Supervised pretraining is not feasible in bioacoustics due to limited datasets. The largest publicly available labeled bioacoustic dataset is arguably the Animal subset of *Audio set* [25], with 112.6 h across 40 758 10 s samples. However, *Audio set* is weakly-labeled [26], is based on YouTube videos that do not reflect realistic bioacoustic recording scenarios, is heavily dominated by recordings of domestic animals and birds ($\approx 75\%$), and is still significantly shorter than the smallest pretraining corpus in human speech recognition, Librispeech (940 hours) [27]. Furthermore, CLR presents conceptual challenges with sparse and unbalanced bioacoustic data, as sparsity hinders effective negative sampling [28, 29]. Despite these obstacles, ViTs have been introduced to bioacoustics [30–35], where approaches range from no pretraining [31, 32] to various pretraining strategies, including web-scraped human speech [35], human language audio-caption pairs [34], pretraining on ImageNet [30, 36], or repurposing pretrained CNNs from *Audio set* [25] as a pre-transformer feature extraction step [33]. As of now, pretraining a transformer model with bioacoustic data is still an open problem.

Consequently, deep learning in bioacoustics is facing a double-edged challenge: the inherent constraints of spectrograms and the conceptual problems of prevailing pretraining strategies in computer vision.

We address both issues by releasing *animal2vec* and *MeerKAT*; *animal2vec* is a framework for training animal call recognizers from raw waveforms containing sparsely distributed calls with non-uniformly distributed call types. Features are extracted from the pressure waveforms using a learned set of SincNet-style filterbanks [37] and a transformer encoder [16, 38].

MeerKAT is a 1068 h large-scale dataset containing data from audio-recording collars worn by free-ranging meerkats (*Suricata suricatta*) at the Kalahari Research Centre, South Africa

[39], of which 184 h are labeled with twelve time-resolved vocalization-type ground truth target classes, each with millisecond resolution. *animal2vec* is conceptually simple, excels with noisy and sparse datasets, achieves state-of-the-art performance, is capable of learning from limited training data (few-shot learning), and provides temporal and spectral interpretability. The labeled 184 h *MeerKAT* subset exhibits realistic sparsity conditions (96 % background-noise or other signals and 4 % vocalizations), dispersed across 66 398 10-second samples, spanning 251 562 labeled events and showcasing significant spectral and temporal variability, making it the first large scale reference point with real-world conditions for benchmarking pretraining and finetune approaches in bioacoustics deep learning.

We release all the code and pretrained models under an MIT license [40] at our GitHub [41], and the *MeerKAT* dataset under a Creative Commons BY-NC license [42] at the Max-Planck data repository Edmond [43].

Our work: (i) paves the way to adapt and specialize next-generation transformer models to the domain of bioacoustics using the unified *animal2vec* framework, (ii) allows researchers with only little labeled data to classify large amounts of challenging data, and (iii) introduces the first bioacoustic benchmark to evaluate large-scale pretrain/finetune approaches under realistic sparsity and class balancing conditions using *MeerKAT*.

2. Materials and Methods

2.1. The *MeerKAT* dataset

2.1.1. Recording and label availability

Recording and labeling a large-scale dataset is a large-scale endeavor The compilation of *MeerKAT* reflects an extensive collaborative effort by researchers and students (see Acknowledgements) who diligently recorded, labeled, and validated the dataset over an extended period.

The data were collected during two field seasons (Aug-Sep 2017 and Jul-Aug 2019) at the Kalahari Research Centre in South Africa. Meerkats are a social mongoose species native to the arid parts of southern Africa. Meerkats forage throughout the day by digging in the ground for prey, remaining cohesive with their group mates while moving within their territory. They use vocalizations to mediate a variety of social behaviors, and their vocal repertoire has been extensively characterized [44, 45].

Overall, 2521 h of audio has been recorded in 1284 files. The majority of the audio (2269 h in 756 3-hour-long files) originated from acoustic collars (Edic Mini Tiny+ A77, Zelenograd, Russia, which sample at 8 kHz with 10 bit quantization) that were attached to the animals (41 individuals throughout both campaigns), where each file corresponds to a recording for a single individual and day. The remainder of the dataset (252 h in 528 files of varying length) was recorded using Marantz

PMD661 digital recorders (Carlsbad, CA, U.S.) attached to directional Sennheiser ME66 microphones (Wedemark, Germany) sampling at 48 kHz with 32 bit quantization. When recording, field researchers held the microphones close to the animals (within 1 m). The data were recorded during times when meerkats typically forage for food by digging in the ground for small prey.

Labeling was done to cover as many different files from as many days and individual meerkats as possible. In total, 325 files were partially labeled (at least 1 h, but not the full file to cover more files), of which 278 contain audio from collars and 47 from directional microphones.

MeerKAT contains the full audio of these 325 files, amounting to 1068 h, released as 384 592 10-second samples. The labeled subset has a total length of 184 h spread across 66 398 10-second samples. This subset is ground-truth-complete; all call and recurring anthropogenic events in this 184 h are labeled. All 10-second samples have been standardized to a sample rate of 8 kHz with 16-bit quantization, where downsampling was done using Torchaudio's resample method [46] with a Kaiser window [47] and a low-pass filter width of 8 ms. This yields a total dataset size of just under 59 GB (61 GB including the label files). While the sampling rate of 8 kHz is sufficient to capture the majority of meerkat vocalization frequencies (the first two formants are below the Nyquist frequency of 4 kHz [48]), the total dataset size is comparatively small, making MeerKAT easily accessible and portable despite its extensive length. By agreement with the Kalahari Research Centre (KRC), we have made these data available in a way that can further machine learning research without compromising the ability of the KRC to continue conducting valuable ecological research on these data. Consequently, the filenames of the 10-second samples have been randomly sampled, and their temporal order and individual identity cannot be recovered, but can be requested from us. The order and identity of the files are not needed in order to recreate the results of this work.

The overall structure of MeerKAT, having a huge unlabeled and a large fully-labeled subset originating from the same pool of audio files, make it an ideal test-bed for pretraining/finetune approaches in bioacoustics.

2.1.2. Label structure and statistics

The labels in MeerKAT reflect over twenty years of research

In total, eight *vocalization* classes and three *miscellaneous* classes were identified. The vocalization classes are: *close call* [49], *short-note call* [50, 51], *social call* [44], *alarm call* [52], *aggressive call* [50], *move call* [50, 53], *lead call* [53], and *other call* (see also [44, 45] for a general overview on meerkat vocalizations). Meerkats can produce some calls that do not fit well into the set of described calls. These calls are frequently hybrid calls that bear similarity to multiple call types, or are simply too rare to have their own category. Such calls are labeled as *other call* within MeerKAT. The three

miscellaneous classes are for non-call events. The *synch* and *beep* events are generated by a GPS clock that was used to synchronize acoustic streams to one another across animals for the purposes of the behavioral study for which the data were collected (see 3.1.3 in [2]). The eating label indicates chewing noises from a successful foraging event. In addition to the vocalization and miscellaneous classes, a superordinate class called *focal* is used to indicate when a call was produced by the focal animal wearing the collar as opposed to a nearby conspecific. Trained analysts made this decision based on relative intensity of calls, changes in the frequency spectrum, and contextual information (see also supplemental information in [54]). Each 10-second file has an accompanying HDF5 label file [55] that lists label categories, start and end time offsets (s), and a focal indicator.

MeerKAT is *multi-class* and *multi-label*, which means that ground-truth labels may overlap. The temporal resolution of all labels is in the few ms range (12 ± 7 ms inter-rater reliability [56]). All classes, as well as the distribution of the call durations, are shown in figure 1 a).

MeerKAT is intra- and inter-class unbalanced, sparse, spectrally rich, and dirty MeerKAT is a highly unbalanced and sparse dataset in terms of event-occurrence, event-lengths, and class balance. While the labeled subset covers almost 184 h, the total duration of all labeled parts is only 13.2 h (7.2%). Moreover, considering only the vocalization events, this reduces to 7.8 h (4.2%).

For example, while the Short-note class is overrepresented in terms of occurrence (27% of all counts), the median length is only 37 ms, making it underrepresented in terms of duration (4% of the total duration, whereas 9% would be expected in a balanced dataset). On the other end, the synch signal is an artificial voice signal from a GPS clock whose median duration is 1258 ms, making it account for 28.1% of the total duration of all events but only for 4% of all occurrences. Furthermore, the rarest five classes (other call, alarm call, aggressive call, move call, lead call) added together account for only 14% of the occurrences and 12% of the total duration. Consequently, MeerKAT is two-fold unbalanced: The significant differences in the temporal and occurrence-wise distributions can make a single class over- and underrepresented simultaneously (intra-class balance) and make reasoning about a particular class's abundance, compared to other classes, very complex (inter-class balance). Therefore, there is no clear path to implement existing approaches to handle imbalance in datasets [57, 58].

Figure 2 provides concrete examples plotted as Mel spectrograms in dB scale for (a) a representative stream of audio and (b) the individual classes in MeerKAT. a) shows four alarm call events covered by a varying amount of spectrally broad, ultra-short, and non-stationary noise patterns originating from the meerkats foraging for food by digging in the ground or bumping their collars into obstacles. Noise patterns such as these permeate the majority of MeerKAT. b) shows the spectral

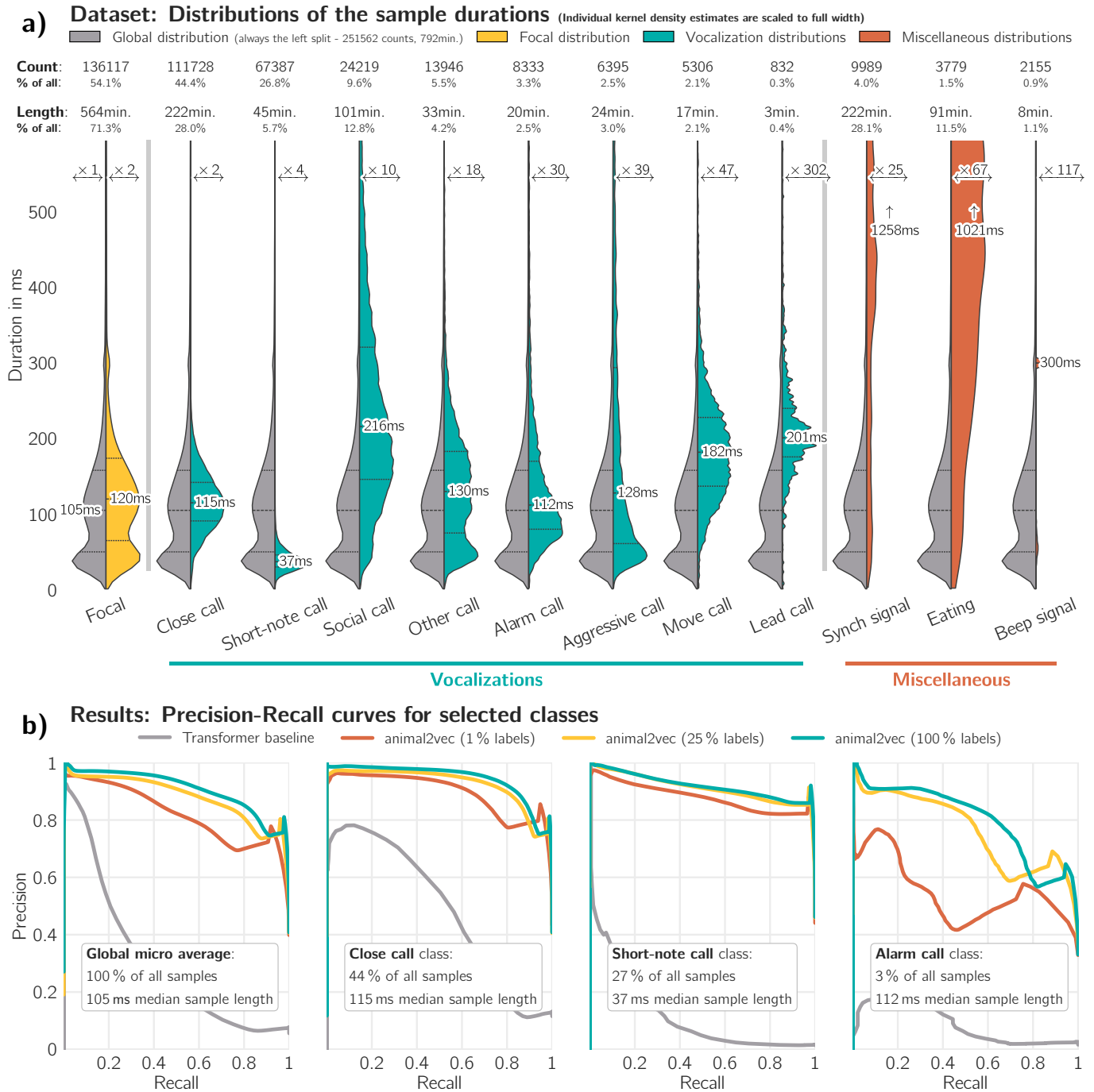


FIG. 1. The statistics of the meerkat dataset and precision-recall curves of the presented classifier. a) shows the temporal distributions of all MeerKAT classes in 12 violin plots. Each category shows kernel density estimates of duration for the class (colored splits on the right). The global distribution across all categories is shown in gray on the left of each plot to make clear how the label durations of each category relate to the dataset overall. All splits are scaled to full width, where the scaling multiplier is shown at the top of each split, as the number of examples for each category varies considerably. In each split, dashed lines show the 25th, 50th, and 75th percentile, where the 50th percentile (median) value is written next to its dashed line. In addition, the event-count, the total length in minutes, and the percentage with respect to all counts/total length are displayed at the top of each plot. b) shows four precision-recall curves for (i) the global micro average, and the (ii) close call, (iii) short-note call, and (iv) alarm call class. Results of animal2vec using 1%, 25%, and 100% of the training data are in red, yellow, and teal, respectively, and the baseline results are in gray. Overlays within each subplot show statistics about the occurrence-wise percentage share and the median duration of all events in this class.

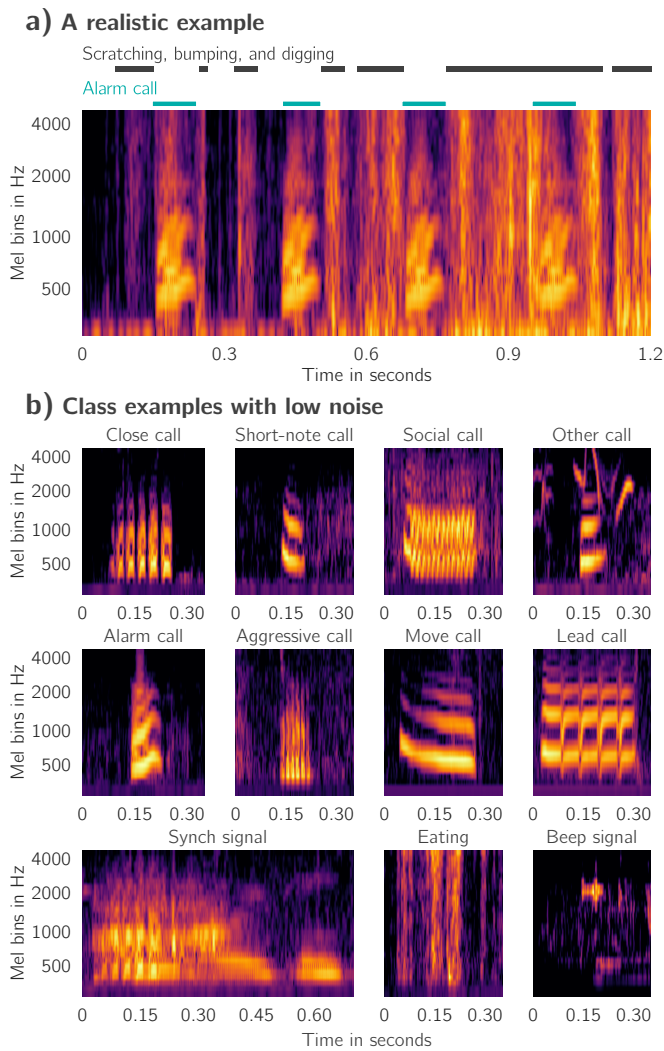


FIG. 2. Example Mel spectrograms for a representative audio snippet and for each class.

variability between classes, where the examples shown do not represent the overall data quality but reflect ideal candidates. Ultimately, MeerKAT makes a formidable benchmark for exploring sparsity, noise-resistance, and imbalance in bioacoustics, containing events that are rare or plentiful, long or short, artificial or natural, temporally and/or occurrence-wise sparse, and spectrally rich, all while being covered in a challenging amount of spectrally broad, ultra-short, and non-stationary noise patterns.

MeerKAT comes with 5-fold stratified multi-label cross-validation finetune/evaluation splits Along with the 10-second audio files and their labels, we release manifest files containing the filenames of the 10-second splits used to build each experiment’s finetune and evaluation splits. We conducted four experiments: (i) A full finetuning using all training data, (ii) two few-shot experiments, and (iii) one generalizability study with a holdout file not used for pretraining or finetuning. All four experiments’ finetune and evaluation splits are

produced using stratified 5-fold multi-label cross-validation [60]. Final results are averaged and provided along with their standard deviation.

Our strategy to produce (i) and (ii) was to produce the five folds of finetune and evaluation splits in the first step using all available data. This produces the scenario in (i). Then, for each of the five finetune splits, we construct two stratified few-shot versions using 1% and 25% of the data, keeping the evaluation split identical for all scenarios. This produces the scenario in (ii) and yields a total of 15 finetune and five evaluation splits: Five folds for each of the three finetune splits (using 1%, 25%, and 100% of the training data) and one evaluation split for each fold.

We publish this set of manifest files along with MeerKAT to ensure reproducibility and comparability of different approaches when using MeerKAT and to provide low-threshold access to this extensive evaluation routine.

Table I b) holds the average sample sizes for all experiments except the generalizability study. When averaging across all five folds, the standard deviation is given in smaller brackets next to each value.

For the holdout generalizability study (iii), we randomly selected 62 ($\approx 20\%$) full files of the 325 base files in MeerKAT and used all labeled 10 s-segments within them to produce a 33.5 h evaluation split. The data used in this evaluation split are not used during pretraining or finetuning. The results for the generalizability study and their discussion are in section 3.1.2.

2.2. The NIPS4Bplus dataset

NIPS4Bplus is a diverse multi-label small-scale dataset

The NIPS4Bplus dataset is an openly available and densely annotated multi-class and multi-label birdsong audio dataset initially created for the NIPS4B 2013 challenge [61]. It contains 687 recordings of 51 bird species categorized into 81 classes (Multiple bird species produce a vocalization and a song signal). Song Meter SM2BAT recorders using SMX-US microphones (both manufactured by Wildlife Acoustics, Maynard, MA, U.S.) were placed in 39 locations across France and Spain. The total duration of all field recordings is 30 h, where the final dataset release has a duration of 3435 s in 687 5 to 6-second files (≈ 1 h) [12], sampled at 44.1 kHz with 16 bit quantization. 1104 s (33.7%) of the total duration are bird vocalizations or songs, of which 184 s contain overlapping signals. The selected recordings are chosen to maximize diversity across bird species, recording location, and signal type. A full description of the dataset is available in [12].

We include the NIPS4Bplus dataset in this work to be able to benchmark our model with other approaches using the same dataset [62, 63] but resample the entire dataset to 32 kHz with 16 bit quantization to strike a balance between the computational cost of our model and the necessary sampling rate to capture all relevant features. The computational cost of trans-

TABLE I. Class-wise dataset statistics and results. a) shows the average precision scores (AP) [59] of each model, where the underscores indicate the training sample size during finetuning. *Transformer baseline* uses 100% of the training samples for finetuning. The strongest result per class is in bold letters. The two bottom rows show the micro- and macroaverage across all classes except *Focal*. b) shows the training and evaluation split sample sizes used for finetuning. The standard deviation across the stratified multilabel 5-fold cross validation routine [60] is given in smaller brackets next to each value.

a)	Average precision scores [59]					b)	Sample sizes			
	Transformer baseline[38]	animal2vec					Evaluation	Training		
		100 %	1 %	25 %	100 %			-	1 %	25 %
% Training labels										
Focal	0.59 ₍₂₎	0.86 ₍₁₎	0.92 ₍₁₎	0.94 ₍₁₎	24594 ₍₂₈₀₎	983 ₍₂₈₎	24650 ₍₁₃₅₎	98520 ₍₂₈₀₎		
Vocalizations										
Close call	0.49 ₍₁₎	0.90 ₍₂₎	0.93 ₍₂₎	0.94 ₍₁₎	22418 ₍₁₅₃₎	907 ₍₄₁₎	22342 ₍₁₃₇₎	89310 ₍₁₅₃₎		
Short-note call	0.14 ₍₁₎	0.88 ₍₁₎	0.91 ₍₁₎	0.92 ₍₁₎	13336 ₍₁₅₈₎	522 ₍₄₀₎	13505 ₍₁₃₉₎	54051 ₍₁₅₈₎		
Social call	0.30 ₍₂₎	0.65 ₍₁₎	0.79 ₍₁₎	0.84 ₍₁₎	4788 ₍₈₁₎	207 ₍₁₄₎	4847 ₍₄₂₎	19431 ₍₈₁₎		
Other call	0.07 ₍₁₎	0.33 ₍₂₎	0.43 ₍₁₎	0.50 ₍₂₎	2754 ₍₆₇₎	114 ₍₁₈₎	2799 ₍₅₈₎	11192 ₍₆₇₎		
Alarm call	0.03 ₍₁₎	0.57 ₍₁₎	0.77 ₍₁₎	0.80 ₍₁₎	1649 ₍₁₁₈₎	71 ₍₁₂₎	1704 ₍₇₄₎	6684 ₍₁₁₈₎		
Aggressive call	0.09 ₍₁₎	0.54 ₍₂₎	0.62 ₍₁₎	0.71 ₍₂₎	1214 ₍₅₈₎	50 ₍₁₅₎	1338 ₍₂₈₎	5181 ₍₅₈₎		
Move call	0.09 ₍₂₎	0.59 ₍₁₎	0.53 ₍₂₎	0.61 ₍₁₎	1080 ₍₂₃₎	42 ₍₆₎	1071 ₍₃₄₎	4226 ₍₂₃₎		
Lead call	0.01 ₍₁₎	0.41 ₍₁₎	0.39 ₍₂₎	0.50 ₍₁₎	165 ₍₁₀₎	8 ₍₁₎	174 ₍₁₂₎	667 ₍₁₀₎		
Miscellaneous										
Synch signal	0.91 ₍₁₎	0.89 ₍₁₎	0.96 ₍₁₎	0.98 ₍₂₎	1999 ₍₂₎	80 ₍₀₎	1997 ₍₁₎	7990 ₍₂₎		
Eating	0.12 ₍₁₎	0.59 ₍₁₎	0.83 ₍₂₎	0.87 ₍₁₎	760 ₍₁₀₎	31 ₍₂₎	754 ₍₁₁₎	3019 ₍₁₀₎		
Beep Signal	0.26 ₍₁₎	0.74 ₍₁₎	0.77 ₍₂₎	0.80 ₍₁₎	430 ₍₅₎	18 ₍₁₎	431 ₍₄₎	1725 ₍₅₎		
Macroaverage	0.26 ₍₁₎	0.66 ₍₁₎	0.74 ₍₁₎	0.78 ₍₁₎						
Microaverage	0.30 ₍₁₎	0.83 ₍₁₎	0.88 ₍₁₎	0.91 ₍₁₎						

former models scales quadratically with longer input sequences [16], which is directly proportional to the sampling rate. However, we found a Nyquist frequency of 16 kHz sufficient for our experiments as the fundamental frequencies of birds rarely exceed 12 kHz [64]. Furthermore, we pad all recordings to 6 s length and store them in the same format as MeerKAT. We provide scripts in our repository to reproduce this processed version of NIPS4Bplus; see *Code availability* statement.

To finetune with NIPS4Bplus, we pretrain with unlabeled xeno-canto data Transformer-based architectures lack the inductive bias found in convolutional-based models; as such, learning from small-scale datasets is prohibitively more difficult [65]. Consequently, and since NIPS4Bplus is a birdsong dataset, we pretrained our model with data from the xeno-canto database, which is a large citizen science project for recordings of bird vocalizations and shares enough similarity with the NIPS4Bplus dataset to provide a good starting point for downstream finetuning. We use the data provided as part of the Cornell Birdcall Identification Kaggle challenge [66], with additional xeno-canto data from [67] and [68]. This pretraining dataset has no overlap with the NIPS4Bplus dataset and a total length of approximately 700 h, where we cropped/padded all files to have a maximal length of 6 s. Files with a duration

longer than 6 s were split into multiple samples. We resampled all files to 32 kHz with 16 bit quantization. We provide scripts in our repository to reproduce this pretraining corpus; see *Code availability* statement. We do not use the label information from this pretraining dataset at any time.

2.3. animal2vec pretraining

2.3.1. Concept

Pretraining is necessary, but the dominant schemes are not ideal for bioacoustics In the last decade, there has been no training scheme more successful across all data modalities than the self-supervised pretrain/finetune scheme [24, 69, 70]. In general, self-supervised learning is a training paradigm in which a generalist model is trained using an artificial supervisory task created from the data without using any ground truth [24].

Currently, contrastive-learning-based (CLR) pretraining is the dominant scheme in computer vision [22, 23, 71–73] and audio processing [74, 75], whereas generative methods (learning by reconstructing), either autoregressive [76] or bidirectional mask-prediction [77–79], yield state-of-the-art results in natural language processing.

However, these approaches are not conceptually well suited to handle bioacoustic data. CLR-based methods suffer from inefficient negative sampling with sparse and unbalanced datasets [28, 29, 80], and generative pretraining diverges faster when faced with sparse and noisy data [81, 82].

animal2vec is a mean teacher self-distillation process for sparse data An alternative pretraining method is to use a distillation process [83] with no labels, called mean teacher self-distillation [38, 84–87], which is known to be a noise-robust learning scheme [88]. Distillation, in general, is the notion of transferring knowledge from a teacher to a student model, whereas mean teacher self-distillation is to update only the student model via gradient descent and let the teacher model track the student’s weights using an exponentially moving average (EMA).

Grill and colleagues [85] provide intuition for why this process works. They randomly initialized two models: A fixed non-trainable (teacher) and a trainable model (student). The teacher received the input, and the student was trained to regress the embeddings produced by the teacher. Evaluating the student model, after training, on ImageNet [36] using the linear-evaluation protocol [89, 90] resulted in 18.8% top-1 accuracy, whereas the fixed teacher scored 1.4%.

Consequently, it is possible to obtain improved embeddings from the embeddings of an inferior model. Intuitively, in the mean teacher self-distillation regime, the student learns an improved representation by regressing the teacher’s output, which in return improves the teacher, as its weights are updated by tracking the student’s ones. This is a feedback loop and sequentially increases the performance of both models over the course of the pretraining. Afterward, only the student model is used for subsequent finetuning.

In *animal2vec*, we use a self-distillation framework similar to *data2vec 2.0* [38], where the model is treated as three components: A single feature extractor and two contextualizing networks (student and teacher), see figure 3. The feature extractor is domain-specific, and the two contextualizing networks are domain-agnostic transformer architectures [16]. The feature extractor receives the batch of input samples and produces a fixed-size initial representation that is fed to the two contextualizing networks. The teacher receives the full initial representation from the feature extractor, and the student receives the unmasked timesteps from a masked embedding (see figure 3 and the following subsection). The teacher produces a target embedding, and the student produces a prediction embedding. The loss function during pretraining is then a mean-squared-error regression to match the prediction and the target; see section 2.3.3 for more details.

2.3.2. Masking and regularization

Bioacoustic data requires strong regularization Regularization alters the model architecture, the input data, or the training process to increase robustness against out-of-distribution

samples, noise, label imbalance, and overfitting [88]. Using strong regularization has a rich history in bioacoustics since natural sounds inherently present immense variability between species, individuals, and environments. Models in bioacoustics can easily overfit to training data, struggling to generalize to new scenarios. [18, 91–93].

For *animal2vec* pretraining we use decoupled weight decay [94], dropout [95], and layer normalization [96] in all layers. We augment the input audio files using the stochastic A-weighted input mixing in between-classes-learning [97] (BCL), as shown in figure 3. We reduce the window length in BCL from 100 ms to 50 ms to calculate the A-weighted sound pressure levels to account for the fact that animal vocalizations act on a shorter timescale than the generic sound input BCL was designed for.

However, the most critical regularization technique during the *animal2vec* pretraining stage is the stochastic strategy used to mask the embeddings input to the student model, see figure 3, where we use the same ruleset as in [38, 74, 87]. First, the masking routine randomly selects a proportion (specified by the probability parameter p) of the total timesteps in the embedding space. These act as starting points for the masked spans. Then, starting from each selected timestep, the model masks a consecutive span of steps (the length of this span is determined by the mask length parameter M) by filling the span with randomized values from a normal distribution. Masked spans can overlap, where the union of the overlapping regions is then used for masking. Higher values for p select more start frames, and higher values for M mask longer spans, starting from these start frames.

Humans sound different than meerkats Most research on pretraining using mean-teacher self-distillation and raw audio as input is concerned with human speech audio [38, 87]. However, reconstructing masked timesteps is easier from their surroundings in human speech than in bioacoustics. Humans have rich vocal expressions where information is correlated over longer stretches of time compared to meerkats and most other non-human animals. Furthermore, sparsity is much less pronounced in human speech data than in bioacoustic datasets [18, 38].

The best set of parameters for human speech is $p = 0.065$ and $M = 10$ [38, 74, 87], which results in 49% of all timesteps masked, where the most frequent span length (the mode in the red mask length distribution in figure 4) is 50 ms. This set of parameters would almost always mask a complete short-note call (median duration of 35 ms, see figure 1 a) when a starting point was selected near such a call. It would expose long stretches of noise to the teacher as only 49% of all timesteps are masked, but over 96% of MeerKAT contains various challenging noise patterns.

Therefore, the masking strategy in *animal2vec* selects more starting points ($p = 0.150$) with shorter mask lengths ($M = 2$). This way, almost 96% are masked, but the mode of the mask

animal2vec pretraining scheme and model

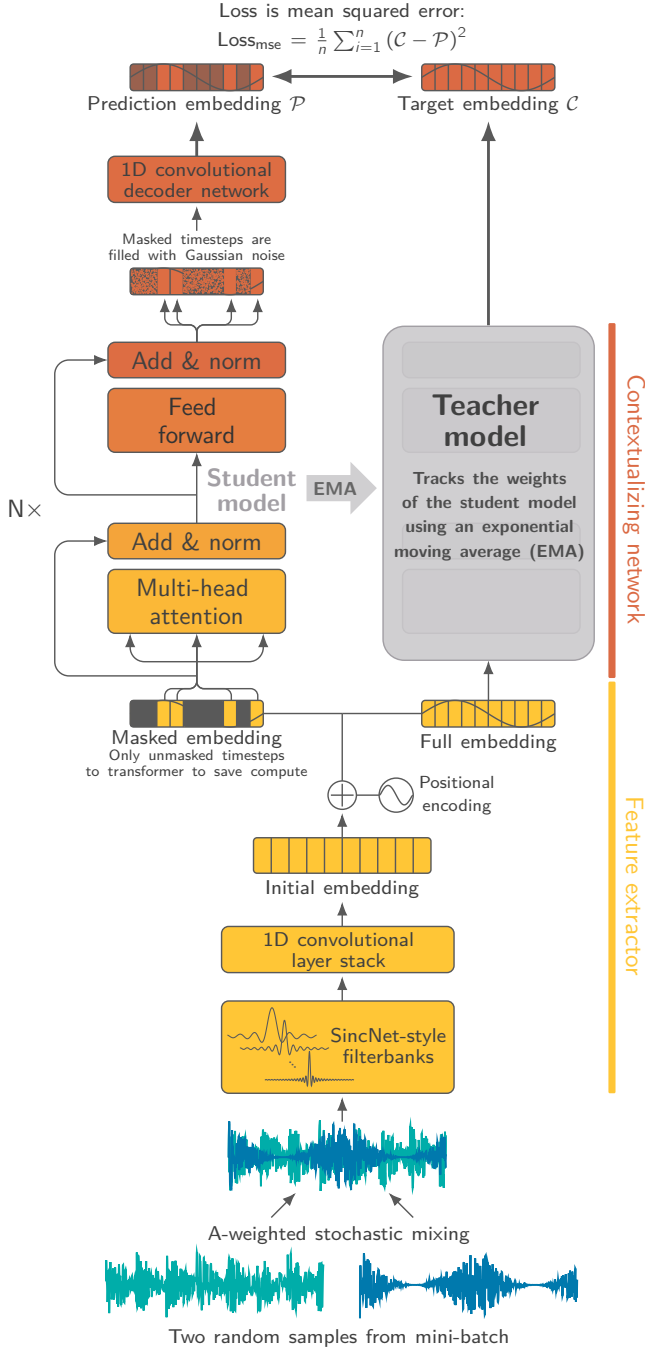


FIG. 3. animal2vec pretraining schematic.

length distribution is 22 ms (the yellow mask length distribution in figure 4). We ablate our choice for p , M , and the BCL window length in section 3.1.2. Ablation studies in machine learning test the importance of different model components by systematically removing them and observing the impact on performance.

2.3.3. Architecture and technical details

animal2vec uses an efficient transformer architecture with a convolutional decoder for pretraining We follow [38, 74, 87] and use large transformers [16] for the student and the teacher with 16 layers (N in figure 3) and 16 attention heads with an embedding dimensionality of 1024. We use a custom feature extractor tailored for bioacoustic data that employs SincNet-style filterbanks [37] and a stack of 1D convolutional layers that learns a downsampling to an effective sample rate of $f_{\text{sr, eff}} = 200$ Hz. The whole feature extractor module (see yellow segment in figure 3) has a receptive field size of 46 ms. Our Sinc module differs from [37] in that it uses no max pooling, a custom activation function, layer normalization, and smaller Sinc filters (8 ms receptive field size, kernel size $k = 63$ over 31 ms, $k = 251$ in [37]). We choose a kernel size k according to $k = \lfloor f_{\text{sr}}/126 \rfloor$, where f_{sr} is the sample rate of the input. This rule fixes the spectral resolution to 126 Hz and results in a kernel size of 63 for MeerKAT 253 for NIPS4Bplus. A spectral resolution of 126 Hz was empirically found to work best for both datasets.

Research on activation functions has shown that early convolutional layers benefit from near-linear parametric activation functions as these often act as bandpass filters [98]. Therefore, we use a custom version of the Swish activation function [99] (sometimes called SiLU with learnable β parameter [100]) called PSwish with additional learnable parameter α of the form: $h(x) = x \alpha \sigma(\beta x)$, where σ is the sigmoid function. We set the shape of α and β to the number of Sinc filters, initialize them with $\alpha = 2$ and $\beta = 0$, and exclude α and β from the weight decay regularization as smaller activation parameters are not necessarily beneficial in parametric activations [98]. This way, PSwish is a linear activation when training starts but becomes an individual non-linearity for every filter throughout training.

As in [38], we embed only unmasked timesteps with the student network, use a learned positional encoding [101], and implement a 1D convolutional decoder to reconstruct the prediction embedding, where the masked timesteps are filled with Gaussian noise prior to passing it to the decoder [101]. Furthermore, we re-use the teacher representation as target for multiple masked versions of the input sample, this is called multi-mask training [38]. Passing only unmasked timesteps to the student and re-using the teacher for multi-masking improves efficiency and reduces the computational cost significantly [38] since the computational complexity of transformer networks scales quadratically with their input length [16].

The teacher network tracks the student weights using an EMA update rule, where we use the implementation and parameters in [38, 87].

The output of our model consists of likelihood estimates with a resolution of 200 Hz. A full schematic of the model in pretraining mode is shown in figure 3. The final model has 315M trainable parameters. We train for 100 epochs using

the decoupled Adam optimizer (weight decay of 0.01) [94], a cosine learning rate schedule [102], linear warmup for 10 000 steps, a final learning rate of 1×10^{-4} , gradient clipping of 1 [103], and a batch size of 1020 s on four NVIDIA A100-SXM4-80GB GPUs for 20 d. The code is written in PyTorch [104] using the fairseq framework [105]. The pretraining parameters for all settings can be found in table V in the appendix.

We estimate that our setup consumed 3200 kWh (the typical yearly consumption of a German household [106]) with a carbon footprint of approximately 1400 kgCO_{2,eq.} (average emission factor of 2023 for Germany is 400 gCO_{2,eq.} kW⁻¹ h⁻¹ [107]). While the resources to train such a model are expensive, leased resources such as using Google Cloud tensor processing unit (TPU) v5p chips are capable of pretraining our model for a more modest cost (about \$500 at the time of writing) and reduce the carbon footprint significantly [108]. In addition, researchers can already use our MeerKAT- or xeno-canto-pretrained animal2vec models to finetune on their custom downstream tasks.

2.4. Finetuning

Strong regularization to tackle sparsity and a self-weighted loss to address label imbalance are critical For finetuning, we mostly follow the approach in [38, 74, 87]. We discard the teacher and the 1D convolutional decoder network (see figure 3) and freeze the weights of the feature extractor. We add a classification head containing a sigmoid-activated linear projection layer and perform a warm-up phase for 10 000 steps, where the student weights are also frozen. The warm-up phase aligns the randomly initialized classification head with the rest of the model. Prior to the classification head, we average the embeddings from all transformer layers rather than just using the output of the last layer; this has been shown to improve results in human speech recognition [87].

After the warm-up phase, we unfreeze the student model and finetune the classification head along with the student model for the remainder of the training. To account for the label imbalance in MeerKAT, we use the focal criterion [109] as opposed to cross entropy as loss function. Focal loss adds a regularization term of the form $(1 - p_t)^\gamma$ to the cross entropy, where p_t is the model’s estimated probability for observing a particular class - the model’s likelihood. Setting γ to a positive number reduces the relative difference in loss between examples where the model is confident (high likelihood) and where it is not (low likelihood). This approach penalizes the effort to improve predictions with high likelihood and forces the model to focus on the ones with low likelihood. As during pretraining, we use between-classes-Learning [97] (BCL) with our modified window length for augmenting the input audio, and we mask parts of the input using the same stochastic masking strategy but with fewer masked spans, depending on the finetuning setting (see table V in the appendix). For the MeerKAT (100%) setting, we use $p = 0.0825$ and $M = 4$,

which sets the mode of the mask distribution to 22 ms while 60% of all timesteps are masked. Compared to the pretraining setting, we aim to maintain a masking distribution with a mode duration below the shortest vocalizations in the dataset but mask fewer of total timesteps. The idea of masking during finetuning is not to create an artificial regression task, as during pretraining, but to use masking as a regularization technique. We benchmark our layer averaging strategy, the use of focal loss, BCL augmentation, and masking strategy in an ablation study [110] in section 3.1.2. The finetuning parameters for each setting can be found in table V in the appendix.

2.5. Calculating metrics

We report real-life relevant per-event metrics While our model generates likelihood estimates at a temporal resolution of 200 Hz, we evaluate performance using per-event scores since reporting metrics on a frame level are biased with respect to event lengths. Longer events cover more timesteps and need more predictions than shorter ones. This favors overly positive or, likewise, disfavors overly negative models. We calculate event-based scores where a single event is a single prediction, regardless of the event length. This enables us to report how many calls were correctly identified and how many were missed, rather than focusing on the likelihood of each audio frame. We calculate this as follows:

1. *Event boundary prediction:* We slide a fixed-length average-pooling window across the model’s likelihood output to predict event onsets and offsets within a continuous audio stream. A fixed threshold is applied to binarize the output, generating a step function representing our event boundary estimates.
2. *Intersection-over-union (IOU) calculation:* Using the IOU metric, we measure the overlap between the ground truth event spans and our predictions. Predicted spans without corresponding ground truth events are assigned an IOU of zero.
3. *Final likelihood assignment:* If the IOU for a predicted event exceeds 0.5, the average model likelihood within the predicted span is used as the final scalar likelihood. All reported metrics utilize these final likelihood values.
4. *Error identification:* Ground truth events without predicted boundaries are considered false negatives. Predicted spans lacking a ground truth counterpart, or those with insufficient IOU, are considered false positives.

3. Results & Discussion

3.1. MeerKAT

We selected three classes to highlight the different challenges in bioacoustics compared to human speech We

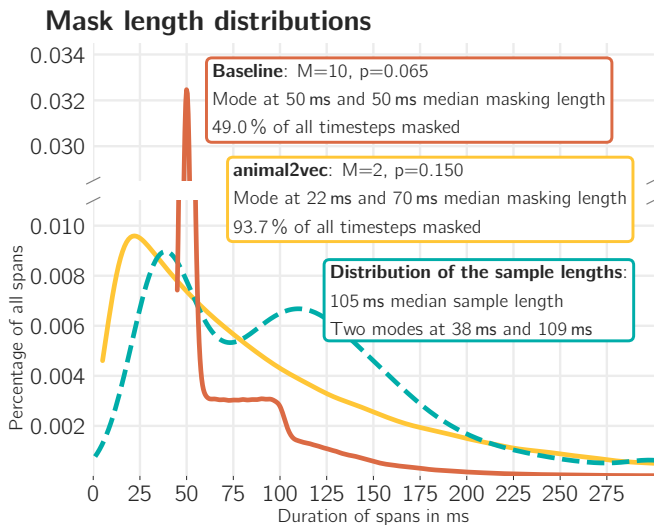


FIG. 4. Mask length distributions of the baseline (solid red line) and our animal2vec model (solid yellow line) during pretraining. For comparison we also show the distribution of the sample lengths (dashed teal line). Modeled after figure 2 in the appendix in [74].

compare animal2vec to the transformer baseline presented in Baevski et al. (2022) [38]. This baseline introduced the pre-training scheme we have adapted to bioacoustics, and achieved state-of-the-art results on the Librispeech speech recognition corpus. It is optimized for human speech but is architecturally close to animal2vec. We chose precision-recall (PR) curves to characterize model performance with the MeerKAT dataset. A PR curve is constructed by plotting precision values on the y-axis against recall values on the x-axis across various likelihood thresholds. Precision describes how accurate the positive predictions are (Out of all predictions, how many are correct), while Recall describes how complete they are (How many events should have been labeled). The likelihood threshold determines the likelihood above which an instance is predicted as belonging to a class (whether a call was detected). By varying this threshold, we can explore the trade-off between the model’s precision and its ability to recall all positive instances. We present PR curves for selected classes and for all three finetuning settings with MeerKAT in figure 1 b) and for the remaining classes in the appendix (see figures 8 to 19). Figure 1 b) provides results in four subplots showing (i) the global micro average, (ii) the close call, (iii) the short-note call, and (iv) the alarm call class. Each subplot holds four PR curves that belong to (i) the transformer baseline (in gray) and (ii - iv) animal2vec in the reduced (1%, 25%), and full (100%) training data finetuning settings (in red, yellow, and teal, respectively). While the global micro average provides a good overview of overall performance, we selected the three vocalization classes to discuss relevant use cases:

1. *The easiest class*: The close call class is the most abundant single vocalization with a representative median

length of 115 ms (compared to 105 ms in MeerKAT).

2. *The shortest class*: While it is the second most abundant vocalization class, the short-note call class has the shortest median length of 37 ms. As such, it is an ideal candidate to assess the model’s performance on very short signals. This is especially interesting as it highlights conceptual differences between bioacoustic and human speech datasets, where the typical phoneme length in the English language is ≈ 100 ms [111, 112].
3. *The rare class*: The alarm call class has a somewhat comparable duration distribution to the close call class (*the easiest class*), see figure 1 a) but is one of the rarest vocalization classes in MeerKAT, which makes it ideal to assess a model’s ability to learn from underrepresented classes.

Furthermore, we use the AP [59] score to assess class-wise performance in the main text in table I a). The AP score is a robust estimator for the area under the PR curve [113] and is computed by averaging the interpolated precision values at evenly spaced recall levels across the entire precision-recall curve.

animal2vec is strong where the baseline is weak and very strong where the baseline is ok animal2vec consistently outperforms the transformer baseline even in the 1% setting (see global micro average in figure 1 b) and AP scores in table I a)). The baseline achieves a precision of 0.5 for recall values below 0.2 (Overall AP score is 0.30), whereas even the animal2vec 1% setting never falls below a precision of almost 0.7 (at recall around 0.8; Overall AP score is 0.83). The models trained using the 25% and 100% finetune splits outperform the baseline and the 1% result by a wide margin (Overall AP scores of 0.88 and 0.91). Their AP scores and precision-recall curves are comparable, indicating that, for the global micro average, a saturation level may have been reached above which improvement is not achievable by merely providing more labeled samples.

The results for the three selected classes in figure 1 b) show the transformer baseline performing reasonably on the close call class (*the easiest class*; AP score of 0.49) but achieving low scores with the Short-note and alarm call class (*the shortest and the rare class*; AP scores of 0.14 and 0.03). animal2vec significantly outperforms this baseline, achieving AP scores of 0.90, 0.88, and 0.57 using 1% of the data and 0.94, 0.92, and 0.80 using 100% of the data. As observed in the global average, results using 25% and 100% of the labels are comparable, indicating a saturation effect, where further improvements are not attainable through more labeling.

We observe this saturation effect for all but three of the four rarest classes (Alarm, Aggressive, and lead calls), see table I a). The move call class is the only rare class where animal2vec was able to achieve a comparable result in the 25% and 100%

Cumulative frequency response of sinc filters

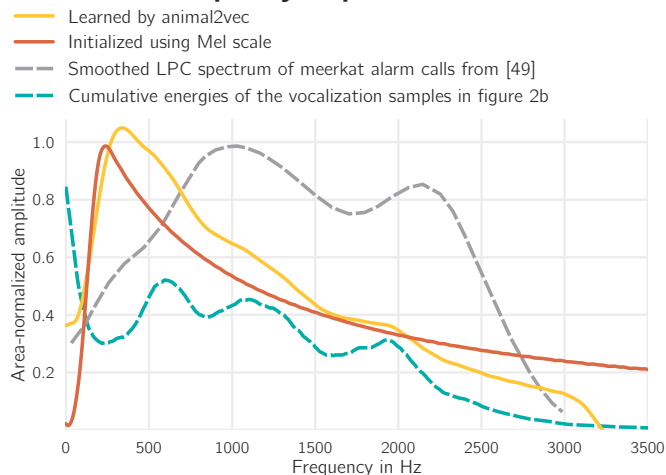


FIG. 5. Cumulative frequency response (CFR) of the SincNet filters learned by *animal2vec* after pretraining (solid yellow) and initialized with the Mel-scale (solid red). For comparison, the 800 Hz cepstral-smoothed linear predictive coding (LPC) spectrum of meerkat alarm calls [48] (dashed grey) and the integrated spectral energies of the vocalization samples in figure 2 b) (dashed teal) are shown. All lines are area-normalized.

setting. We attribute this to the move call class being somewhat easier to predict, having a longer median length of 182 ms (the third longest of all vocalization classes), but being not so rare as the comparably long lead call class, see figure 1 a).

The results for the miscellaneous classes (synch, beep, and eating) are comparable to the vocalization classes, except for the synch signal class. There, the transformer baseline performs almost on par with *animal2vec*, achieving an AP score of 0.91. This is expected as a synch signal is an artificial human voice from a GPS clock saying loudly the current time, see section 2.1.2. The baseline performs well on this class since it was derived for human language [38]. However, even in this case, *animal2vec* (1 %) matches the baseline performance (AP score of 0.89), using only 80 instances throughout finetuning, compared to 7990 in baseline finetuning.

3.1.1. Interpretability of *animal2vec*

As far as neural networks are concerned, *animal2vec* is not quite such a black box *animal2vec*'s decision-making can be understood in the spectral and temporal domain. (i) Spectral importance can be deduced from the cumulative frequency response of the learned sinc filters (much like the analysis in [37]), and (ii) temporal importance can be inferred from the attention maps of our transformer architecture. While there are many variants of attention modules [16, 114, 115], a transformer typically uses the scaled matrix-matrix dot product attention [16] as the dominant information extraction mechanism. First, the matrix-matrix product between the input ($X \in \mathbb{R}^{L \times d}$) and three learnable matrices (Q_w , K_w , and V_w), where $\{Q_w, K_w, V_w\} \in \mathbb{R}^{d \times d}$ is calculated, where L is the

segment length of the input sequence and d is the embedding size of the model. Their output is then referred to as Query ($Q = X \cdot Q_w$), Key ($K = X \cdot K_w$), and Value ($V = X \cdot V_w$), where $\{Q, K, V\} \in \mathbb{R}^{L \times d}$. Then, the matrix-matrix product between the query and the transposed key matrix is passed through a softmax layer, and a final matrix-matrix product is calculated with the value matrix. Concretely:

$$\mathcal{H}(Q, K, V) = \underbrace{\text{softmax}\left(QK^T n^{-\frac{1}{2}}\right)}_{\text{Attention}} V = AV \quad (1)$$

where $\mathcal{H}(Q, K, V) \in \mathbb{R}^{L \times d}$ and n is a scalar normalization constant [16]. The output of the softmax layer is referred to as attention ($A \in \mathbb{R}^{L \times L}$), as it acts as a normalized weighting matrix for the value matrix. So, the whole attention module learns two things: (i) a softmax-normalized weighting matrix and (ii) a projection of the input. The first is called attention matrix A , and the second is the Value matrix. Therefore, the attention matrix (A) provides relevance in terms of how the projection of the input (V) should be passed to the next layer. In practice, a single transformer layer calculates equation 1 M times (Q_w , K_w , and V_w , with $1 \leq w \leq M$), where M is referred to as the number of heads (this is what is called Multi-head attention in figure 3), and a full transformer model has N layers (see the $N \times$ on the left in figure 3). Weights of Q , K , and V are not shared between heads or layers, so a full transformer model has M times N attention matrices A .

For interpreting *animal2vec*'s decision-making in the temporal domain, we show the global average of all A matrices as a heatmap. Concretely, we average across 256 attention maps (16 heads times 16 layers; see table V in the appendix).

Interpreting attention maps is a much-debated topic [116–120]. The consensus is that attention maps often provide excellent and intuitive explanations but sometimes are entirely misleading. Therefore, scientists still need to interpret them cautiously [119]. We follow the nomenclature in [114] and interpret the attention scores not as explanations but as importance. Furthermore, we provide scripts in our repository to extract all attention maps from all heads and layers and the parameters of the sinc module.

***animal2vec*'s frequency response broadly aligns with the frequencies found in meerkat calls**

First, we discuss the spectral interpretability of *animal2vec* via the cumulative frequency response (CFR) of the learned sinc filters (see figure 5).

Both reference curves, the dashed lines in figure 5, show good agreement with each other. The most notable features of the data from [48] are the bimodal structures with nodes at around 1 kHz and 2.2 kHz. This is mostly mirrored by our reference data from figure 2, where the spectral distribution shows a trimodal distribution, with peaks at around 600 Hz, 1.1 kHz, and 2 kHz. Both reference lines decay fast to almost zero

Globally averaged attention map

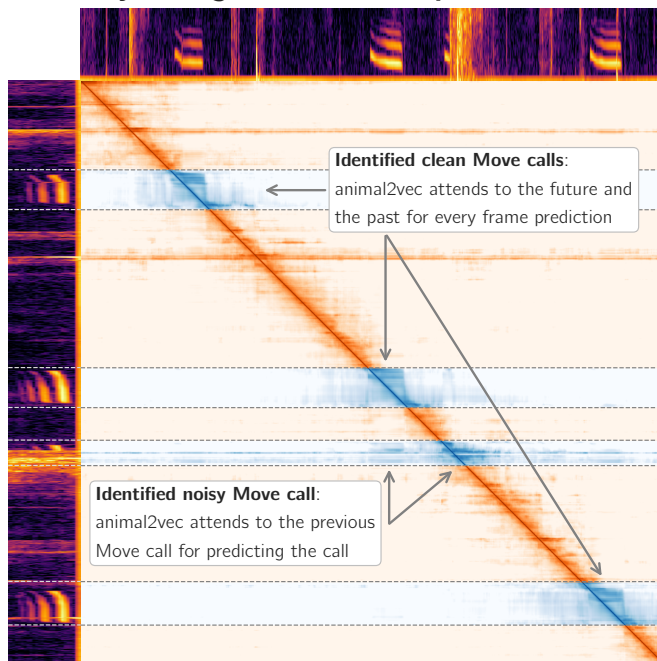


FIG. 6. Globally averaged attention map of a four second segment showing four move calls. Blue stretches surrounded by dashed white lines correspond to onset/offset predictions of animal2vec. An attention map shows the *importance* of every input frame with respect to every other frame. For predicting, animal2vec attends to the immediate past and future of an event, as well as to a previous instance in the case of the noisy Move vocalization.

amplitude between ≈ 2.5 to 3.0 kHz.

The CFR of animal2vec’s learned sinc filters show the strongest response to signals at 355 Hz, an increase by about 115 Hz with respect to the filters initialized using the Mel scale (maximum at 240 Hz). This increase is expected as the Mel scale is derived for human vocalizations which are overall lower in frequency compared to meerkat vocalizations [44, 48]. For frequencies above 500 Hz animal2vec’s CFR largely follows the trimodal structure of the MeerKAT reference data, even mirroring the decline for frequencies between ≈ 2.5 to 3.0 kHz, highlighting that animal2vec learned the relevant frequencies to identify the MeerKAT vocalizations. Since the feature extraction module (the yellow stack in figure 3, including the sinc module) is frozen throughout subsequent finetuning, the presented CFR is learned in the fully self-supervised pretraining, without any labels used.

animal2vec attends to the future, the past, and repeating patterns to predict meerkat calls We discuss temporal interpretability by showing globally averaged attention maps [114] in figure 6. As expected, the dominant feature is the diagonal, which is the importance given by the model to use the current audio frame to make predictions about the current audio frame. Moreover, three observations are striking in figure 6. (i) For the three move calls that are not covered in regions of

TABLE II. Ablation studies for animal2vec compared to the transformer baseline [38], evaluated using the MeerKAT (100%) setting. The microaveraged average precision scores (AP) [59] are obtained after finetuning on the MeerKAT dataset.

	Average precision score [59]
Transformer baseline [38]	0.30
Changes to pretraining as described in [38]:	
• Change feature extractor layout	
\lrcorner $f_{sr, \text{eff}}$ from 50 to 200 Hz	+0.16
\lrcorner SincNet-style filterbanks [37]	+0.03
\lrcorner PSwish instead of LeakyRelu	+0.02
• Change pretraining masking strategy	
\lrcorner Prob. p from 0.0650 to 0.1500	+0.05
\lrcorner Length M from 10 to 2	+0.11
• Between-classes learning [97] (No Targets)	+0.04
Changes to finetuning as described in [38, 74]:	
• Average over all transformer layers	+0.04
• Focal loss [109] instead of cross entropy	+0.05
• Between-classes learning [97]	+0.03
• Change finetuning masking strategy	
\lrcorner Prob. p from 0.0650 to 0.0825	+0.03
\lrcorner Length M from 10 to 4	+0.05
animal2vec	0.91

spectrally broad noise (first, second, and fourth from the top), animal2vec attends to the future and the past of the current audio frame (left and right from the diagonal) for the whole duration of the call. (ii) For the one noisy move call (third from the top), animal2vec attends to the previous move call while predicting the noisy one, and (iii) animal2vec attends to almost all frames in the input sequence for most of the ultra-short, spectrally broad noise patterns.

The most challenging prediction in this segment is the one on the noisy move call. animal2vec did not miss it and achieved an IoU of 0.95 with the ground truth, meaning that the labeling expert estimated onset and offset almost exactly as animal2vec did. Interestingly, animal2vec stops attending to the previous move call when it stops predicting a move call event, although this area is fully buried under noise and other background signals. We hypothesize that the repetition of vocalizations within a sequence can be a proxy for predicting them. This is corroborated by the somewhat extreme example in figure 7 in the appendix. There, a repetition of 15 alarm calls, closely following each other, is shown. animal2vec attends to almost all previous and future calls while predicting the current one. This is also true for the empty stretches in figure 7, where no call was recorded. animal2vec attends to past and future empty stretches when predicting them as negative.

Behavioral research confirms that meerkat vocalizations often

TABLE III. Results on the evaluation split for the holdout generalizability study. The average precision scores (AP) [59] for the baseline and animal2vec. Both models use 100 % of the training samples for finetuning. The strongest result per class is in bold letters. The two bottom rows show the micro- and macroaverage across all classes except *Focal*. Arrows and values in a smaller font next to the results show the change of score with respect to table I.

Average precision scores [59]		
	Transformer baseline[38]	animal2vec (100 %)
Focal	0.54 ↓ _{0.05}	0.93 ↓ _{0.01}
Vocalizations		
Close call	0.47 ↓ _{0.02}	0.93 ↑ _{0.01}
Short-note call	0.14 ↑ _{0.00}	0.90 ↓ _{0.01}
Social call	0.27 ↓ _{0.03}	0.82 ↓ _{0.02}
Other call	0.04 ↓ _{0.03}	0.46 ↓ _{0.04}
Alarm call	0.03 ↑ _{0.00}	0.80 ↑ _{0.00}
Aggressive call	0.10 ↑ _{0.01}	0.69 ↓ _{0.02}
Move call	0.08 ↓ _{0.01}	0.61 ↑ _{0.00}
Lead call	0.01 ↑ _{0.00}	0.51 ↑ _{0.01}
Miscellaneous		
Synch signal	0.89 ↓ _{0.02}	0.98 ↑ _{0.00}
Eating	0.11 ↓ _{0.01}	0.86 ↓ _{0.01}
Beep signal	0.22 ↓ _{0.04}	0.80 ↑ _{0.00}
Macroaverage	0.24 ↓ _{0.02}	0.76 ↓ _{0.02}
Microaverage	0.28 ↓ _{0.02}	0.90 ↓ _{0.01}

appear in repetition patterns within and among conspecific individuals. [121, 122]. Therefore, attending to previous or following repetitions is a proxy for producing predictions.

3.1.2. Ablation and generalizability studies

animal2vec is not more than the sum of its parts, but they are thought-through and plenty Here, we provide an ablation study [110] on every addition we did compared to the baseline presented in [38]. We conducted 13 full animal2vec pretrainings along with their 5-fold cross-validated finetunings (100 %), wherein each ablation, we added a single component present in animal2vec but missing in the baseline. Table II holds the microaverage AP scores for these ablations. The table is organized in the same order in which the components were added.

The changes that produced the most substantial increase in AP are the alteration of the 1D convolutional layer stack to produce an effective sampling rate $f_{sr, eff}$ of 200 Hz instead of 50 Hz (an increase of 0.16), and the changes to the pretraining masking strategy. Changing the masking length M from 10 to 2 yielded an increase of 0.11 AP, and changing the masking probability p from 0.0650 to 0.1500 increased AP by about 0.05.

Importantly, while the change in $f_{sr, eff}$ produced a 16-fold increase in computational complexity, as four times higher $f_{sr, eff}$, results in a 16 times higher complexity in transformers [16], the changes to the masking strategy reduced the complexity 66-fold (the baseline masks 49 %, whereas we mask 93.7 %). Therefore, discussing just the change in $f_{sr, eff}$ and pretraining masking strategy, we increase AP by 0.32 and reduce the computational cost to around 24 % of the baseline.

animal2vec generalizes well For analyzing the generalizability of animal2vec, we derived a leave-out generalizability study, where a number of files in MeerKAT were excluded from pretraining and finetuning but used for evaluation, see section 2.1.2. Table III holds the class-wise AP scores of this experiment. We analyze them in terms of change with respect to the results from I. Observations that stand out are that (i) the baseline generalizes worse, which can be seen from the global averages, and (ii) performance on the other call class is strongly decreased in both models.

- (i) The macroaverage in the baseline is reduced by about 8 % (a drop from 0.24 to 0.21), and the microaverage by about 7 % (a drop from 0.30 to 0.28), compared to 3 % (a drop from 0.78 to 0.76) and 1 % (a drop from 0.91 to 0.90) in animal2vec.
- (ii) The other call class is a collective class for vocalizations that did not fit well into any of the other classes, see section 2.1.2, as such, performance with this class was always significantly lower compared to classes with sample counts on the same order (like the social call class in the 100 % setting, or the short-note call class in the 25 % setting), or having similar median duration (like the aggressive call class that only contains half the amount of samples). As such, performance is expected to deteriorate stronger than in other classes. We observe a relative decrease by about 43 % (a drop from 0.07 to 0.04) in the baseline and about 8 % (a drop from 0.50 to 0.46) for animal2vec - the largest decrease in any vocalization class for both models.

However, the overall performance of animal2vec remains competitive with data that were included in the unlabeled pretraining, where the observed 1 % decrease in microaverage performance could also be explained by statistical fluctuations (The standard deviation of the microaverage in table I is on the same order).

3.2. NIPS4Bplus

We provide Precision, Recall, and F1 scores of animal2vec to compare to results reported in [62, 63] in table IV. While Morfi et al. (2018) [62] reported results from an event detector calculated on a timestep level, Bravo Sanchez et al. (2021) [63] report class-prediction scores for pre-segmented sequences only containing the event to be classified.

TABLE IV. Microaverage classification results on the NIPS4Bplus dataset [12]. The metrics for the models trained on pre-segmented sequences are taken from [63] and the one for binary timestep prediction is the best result from [62], called *WHEN model using MMM loss*. In addition, we provide results for animal2vec’s Onset/Offset/Overlap predictions, using the same methodology described in section 2.5.

	Model	Precision	Recall	F1
a)	Predictions on pre-segmented sequences			
	Densenet121	0.76	0.75	0.76
	Resnet50	0.76	0.74	0.75
	SincNet	0.75	0.73	0.74
	VGG16	0.74	0.73	0.74
	Waveform + CNN	0.72	0.71	0.71
	Onset/Offset/Overlap predictions			
	animal2vec	0.81	0.88	0.82
b)	Binary predictions on timesteps			
	WHEN (MMM)	-	-	0.74
	animal2vec	0.79	0.86	0.82

We compare animal2vec class-wise event-based predictions, see section 2.5, to the results of Bravo Sanchez et al. (2021) [63] in table IV a). Event-based predictions are arguably more challenging than pre-segmented sequences, as onsets, offsets, and timesteps without a signal also have to be predicted.

Furthermore, to enable a comparison with Morfi et al. (2018) [62], we calculate event detection scores from the likelihood output of animal2vec by treating any prediction for any class for a given timestep as an event prediction, which can be found in table IV b). Consequently, we create many false positives with this approach, which, presumably, reduces the reported precision score of animal2vec.

With this in mind, the increase in F1 of about 0.06 compared to Densenet121 (the strongest model in [63]), and 0.08 compared to the WHEN (MMM) model in [62], sets a new baseline on the NIPS4BPlus dataset. The increase is noteworthy compared to the original SincNet model, which utilizes a similar audio frontend to process raw audio. We would like to highlight that our intention with this benchmark is to connect our work to published research and to show that small-scale datasets can be used for finetuning if animal2vec is pretrained with data from a comparable domain. If pretraining is not an option, animal2vec is not recommended since models like the very small SincNet (2.6M parameters) provide a reasonable trade-off between model interpretability, computational complexity, and classification performance.

4. Conclusions

In this work, we present animal2vec and MeerKAT and make them openly available. animal2vec is a self-supervised pretrain-

ing and finetuning scheme that utilizes a custom transformer-based model tailored for bioacoustics, and MeerKAT is the largest publicly-available dataset on non-human terrestrial mammals ever released. The coming age in AI will primarily focus on pretraining/finetuning training paradigms in combination with large-scale generalist models. This transition has so far been challenging for the bioacoustic research community. First, bioacoustics lacks datasets that are large enough to train transformer models with hundreds of millions of parameters and have enough fine-grain ground truth labels to enable effective finetuning. Second, bioacoustics has so far lacked a pretraining/finetuning training paradigm that takes advantage of the novelties in bioacoustics, like the high sparsity, noise corruption, and having raw waveforms as primary data format. This in combination with the focus on ultra-short events of interest make bioacoustics in many regards a more demanding field than human speech recognition.

animal2vec established a new baseline on the MeerKAT dataset, where we showed that it outperforms a comparable transformer architecture devised for human speech by a large margin and that animal2vec is a strong few-shot learner. Using only 1 % of the finetune data, animal2vec surpassed the transformer baseline by more than doubling the baseline AP score (0.30 for the baseline, compared to 0.76 for animal2vec in the 1 % setting). We further showed that our proposed model in animal2vec converges towards a saturation level in performance when using 25 % or more of the available labeled data, indicating that further improvements might not be gained using more ground truth but new conceptual ideas.

To enable a comparison with already published datasets and results, we evaluated a xeno-canto pretrained animal2vec using the small-scale NIPS4Bplus dataset [61], where animal2vec sets a new baseline outperforming currently published results. The MeerKAT dataset we provide here is large-scale with over 1000 h of audio recordings, but it is still portable with just under 59 GB (61 GB including the label files) in size. It has 184 h of millisecond-resolved strong labels of meerkat vocalizations and artificial audio sources buried in a challenging amount of ultra-short and spectrally broad noise patterns. This enables not only analyzing the event detection performance of a model but also its resilience concerning sparsity and noise.

We designed animal2vec as a modular framework whose components can be used as needed depending on the desired application. Our novel feature extraction module can be used as a frontend for other models, and our transformer model can be used with other frontends. Both can be used with other pretraining or finetuning approaches on different datasets or jointly trained with MeerKAT.

The immediate future for animal2vec is (i) to incorporate more data from more species (insects, birds, marine, and terrestrial animals), recording environments (marine, avian), using a more diverse set of recorders (passive acoustic monitoring, different portable recorders using different microphones, audio from

video traps, citizen science data) where challenges like the large variability in different sampling rates need to be solved, and (ii) to include more data modalities like accelerometer and GPS data from next-gen collar tags [2], where animal2vec needs to be enabled to make use of such auxiliary data streams but not to decrease in performance when they are missing. Ultimately, our vision for animal2vec and MeerKAT is for them to be the first stepping stone towards a next-gen reference work, where, in the future, we envision a foundational-level

pretrained animal2vec model that researchers can directly use for finetuning on their data without the need for large-scale GPU facilities.

There is plenty of work ahead of us before we get there. However, it is our great hope that by making everything accessible, fully open, and portable, the research community will strive with us towards this, we believe, shared goal using animal2vec and MeerKAT.

-
- [1] Bradbury, J. W. & Vehrencamp, S. L. *Principles of animal communication* (Sinauer Associates Sunderland, MA, 1998).
- [2] Demartsev, V. *et al.* Signalling in groups: New tools for the integration of animal communication and collective movement. *Methods Ecol. Evol.* (2022).
- [3] Penar, W., Magiera, A. & Klocek, C. Applications of bioacoustics in animal ecology. *Ecol. Complex.* **43**, 100847 (2020).
- [4] Fleishman, E. *et al.* Ecological inferences about marine mammals from passive acoustic data. *Biol. Rev. Camb. Philos. Soc.* **98**, 1633–1647 (2023).
- [5] Laiolo, P. The emerging significance of bioacoustics in animal species conservation. *Biol. Conserv.* **143**, 1635–1645 (2010).
- [6] McLoughlin, M. P., Stewart, R. & McElligott, A. G. Automated bioacoustics: methods in ecology and conservation and their potential for animal welfare monitoring. *J. R. Soc. Interface* **16**, 20190225 (2019).
- [7] Sugai, L. S. M., Silva, T. S. F., Ribeiro, J. W., Jr & Llusia, D. Terrestrial passive acoustic monitoring: Review and perspectives. *Bioscience* **69**, 15–25 (2019).
- [8] Lindseth, A. V. & Lobel, P. S. Underwater soundscape monitoring and fish bioacoustics: A review. *Fishes* **3**, 36–30 (2018).
- [9] Madhusudhana, S. *et al.* Choosing equipment for animal bioacoustic research. *Exploring Animal Behavior Through Sound: Volume 37* (2022).
- [10] Allen, A. N. *et al.* A convolutional neural network for automated detection of humpback whale song in a diverse, long-term passive acoustic dataset. *Front. Mar. Sci.* **8** (2021).
- [11] LOSTANLEN, V., SALAMON, J., FARNSWORTH, A., KELLING, S. & BELLO, J. P. Birdvox-full-night: A dataset and benchmark for avian flight call detection. In *2018 IEEE International Conference on Acoustics, Speech and Signal Processing (ICASSP)*, 266–270 (IEEE, 2018).
- [12] Morfi, V., Bas, Y., Pamuła, H., Glotin, H. & Stowell, D. NIPS4Bplus: a richly annotated birdsong audio dataset. *PeerJ Comput. Sci.* **5**, e223 (2019).
- [13] Ness, S., Symonds, H., Spong, P. & Tzanetakis, G. The orchive: Data mining a massive bioacoustic archive. Preprint at <https://arxiv.org/abs/1307.0589> (2013).
- [14] Wall, C. C. *et al.* The next wave of passive acoustic data management: How centralized access can enhance science. *Front. Mar. Sci.* **8**, 703682 (2021).
- [15] LeCun, Y., Bengio, Y. & Hinton, G. Deep learning. *Nature* **521**, 436–444 (2015).
- [16] Vaswani, A. *et al.* Transformer: Attention is all you need. *Advances in Neural Information Processing Systems 30* 5998–6008 (2017).
- [17] Lin, T., Wang, Y., Liu, X. & Qiu, X. A survey of transformers. *AI Open* **3**, 111–132 (2022).
- [18] Stowell, D. Computational bioacoustics with deep learning: a review and roadmap. *PeerJ* **10**, e13152 (2022).
- [19] Wyse, L. Audio spectrogram representations for processing with convolutional neural networks. In *Proceedings of the First International Conference on Deep Learning and Music*, 37–41 (2017).
- [20] Dosovitskiy, A. *et al.* An image is worth 16x16 words: Transformers for image recognition at scale. In *International Conference on Learning Representations* (2020).
- [21] Khan, S. *et al.* Transformers in vision: A survey. *ACM Comput. Surv.* (2021).
- [22] He, K., Fan, H., Wu, Y., Xie, S. & Girshick, R. Momentum contrast for unsupervised visual representation learning. *Proceedings of the IEEE Computer Society Conference on Computer Vision and Pattern Recognition* 9726–9735 (2020).
- [23] Chen, T., Kornblith, S., Norouzi, M. & Hinton, G. A simple framework for contrastive learning of visual representations. In *International conference on machine learning*, 1597–1607 (PMLR, 2020).
- [24] Liu, X. *et al.* Self-supervised learning: Generative or contrastive. *IEEE Trans. Knowl. Data Eng.* 1–1 (2021).
- [25] Gemmeke, J. F. *et al.* Audio set: An ontology and human-labeled dataset for audio events. In *2017 IEEE international conference on acoustics, speech and signal processing (ICASSP)*, 776–780 (IEEE, 2017).
- [26] Zhou, Z.-H. A brief introduction to weakly supervised learning. *Natl. Sci. Rev.* **5**, 44–53 (2018).
- [27] Panayotov, V., Chen, G., Povey, D. & Khudanpur, S. Librispeech: an ASR corpus based on public domain audio books. In *2015 IEEE international conference on acoustics, speech and signal processing (ICASSP)*, 5206–5210 (IEEE, 2015).
- [28] Jaiswal, A., Babu, A. R., Zadeh, M. Z., Banerjee, D. & Makedon, F. A survey on contrastive self-supervised learning. *Technologies (Basel)* **9**, 2 (2020).
- [29] Chung, Y.-A. *et al.* W2v-bert: Combining contrastive learning and masked language modeling for self-supervised speech pre-training. In *2021 IEEE Automatic Speech Recognition and Understanding Workshop (ASRU)*, 244–250 (IEEE, 2021).
- [30] Gong, Y., Chung, Y.-A. & Glass, J. AST: Audio Spectrogram Transformer. In *Proc. Interspeech 2021*, 571–575 (2021).

- [31] Wyatt, S. *et al.* Environmental sound classification with tiny transformers in noisy edge environments. In *2021 IEEE 7th World Forum on Internet of Things (WF-IoT)*, 309–314 (IEEE, 2021).
- [32] Wolters, P., Sizemore, L., Daw, C., Hutchinson, B. & Phillips, L. Proposal-based few-shot sound event detection for speech and environmental sounds with perceivers. Preprint at <https://arxiv.org/abs/2107.13616> (2021).
- [33] You, L., Coyotl, E. P., Gunturu, S. & Van Segbroeck, M. Transformer-based bioacoustic sound event detection on few-shot learning tasks. In *ICASSP 2023-2023 IEEE International Conference on Acoustics, Speech and Signal Processing (ICASSP)*, 1–5 (IEEE, 2023).
- [34] Robinson, D., Robinson, A. & Akrapongpisak, L. Transferable models for bioacoustics with human language supervision. In *ICASSP 2024-2024 IEEE International Conference on Acoustics, Speech and Signal Processing (ICASSP)*, 1316–1320 (IEEE, 2024).
- [35] Gu, N. *et al.* Positive transfer of the whisper speech transformer to human and animal voice activity detection. In *ICASSP 2024-2024 IEEE International Conference on Acoustics, Speech and Signal Processing (ICASSP)*, 7505–7509 (IEEE, 2024).
- [36] Deng, J. *et al.* Imagenet: A large-scale hierarchical image database. In *2009 IEEE conference on computer vision and pattern recognition*, 248–255 (IEEE, 2009).
- [37] Ravanelli, M. & Bengio, Y. Speaker recognition from raw waveform with sincnet. In *2018 IEEE spoken language technology workshop (SLT)*, 1021–1028 (IEEE, 2018).
- [38] Baevski, A., Babu, A., Hsu, W.-N. & Auli, M. Efficient self-supervised learning with contextualized target representations for vision, speech and language. In *International Conference on Machine Learning*, 1416–1429 (PMLR, 2023).
- [39] The kalahari research centre KRC. <https://kalahariresearchcentre.org>. Accessed: 2024-04-25.
- [40] The MIT license. <https://opensource.org/licenses/mit>. Accessed: 2024-04-25.
- [41] Official GitHub repository for animal2vec. <https://github.com/livingingroups/animal2vec>. Accessed: 2024-04-25.
- [42] Creative Commons Attribution-NonCommercial 4.0 International. <https://creativecommons.org/licenses/by-nc/4.0/>. Accessed: 2024-04-25.
- [43] Schäfer-Zimmermann, J. C. *et al.* MeerKAT: Meerkat Kalahari Audio Transcripts (2024). URL <https://doi.org/10.17617/3.0J0DYB>.
- [44] Manser, M. B. *The evolution of auditory communication in suricates, Suricata suricatta*. Ph.D. thesis, University of Cambridge (1998).
- [45] Manser, M. B., Jansen, D. A. W. A., Graw, B. & le Roux, A. Vocal complexity in meerkats and other mongoose species. *Adv. Stud. Behav.* **46**, 281–310 (2014).
- [46] Resample method of PyTorch 2.2.0. <https://pytorch.org/audio/2.2.0/generated/torchaudio.transforms.Resample.html>. Accessed: 2024-04-25.
- [47] Kaiser, J. F. Digital filters. *Systems Analysis by Digital Computer*, chap. 7, 218–285 (John Wiley and Sons, New York, 1966).
- [48] Townsend, S. W., Charlton, B. D. & Manser, M. B. Acoustic cues to identity and predator context in meerkat barks. *Anim. Behav.* **94**, 143–149 (2014).
- [49] Townsend, S. W., Hollén, L. I. & Manser, M. B. Meerkat close calls encode group-specific signatures, but receivers fail to discriminate. *Anim. Behav.* **80**, 133–138 (2010).
- [50] Collier, K., Townsend, S. W. & Manser, M. B. Call concatenation in wild meerkats. *Anim. Behav.* **134**, 257–269 (2017).
- [51] Demartsev, V., Strandburg-Peshkin, A., Ruffner, M. & Manser, M. Vocal turn-taking in meerkat group calling sessions. *Curr. Biol.* **28**, 3661–3666.e3 (2018).
- [52] Manser, M. B. The acoustic structure of suricates’ alarm calls varies with predator type and the level of response urgency. *Proc. Biol. Sci.* **268**, 2315–2324 (2001).
- [53] Bousquet, C. A. H., Sumpter, D. J. T. & Manser, M. B. Moving calls: a vocal mechanism underlying quorum decisions in cohesive groups. *Proc. Biol. Sci.* **278**, 1482–1488 (2011).
- [54] Demartsev, V., Thomas, M., Manser, M. B. & Strandburg-Peshkin, A. Mapping vocal interactions in space and time differentiates signal broadcast vs signal exchange in meerkat groups. *Phil. Trans. R. Soc. B* (2024).
- [55] The HDF Group. Hierarchical Data Format, version 5. URL <https://github.com/HDFGroup/hdf5>.
- [56] Hallgren, K. A. Computing inter-rater reliability for observational data: an overview and tutorial. *Tutorials in quantitative methods for psychology* **8**, 23 (2012).
- [57] He, H. & Garcia, E. A. Learning from imbalanced data. *IEEE Trans. Knowl. Data Eng.* **21**, 1263–1284 (2009).
- [58] Chawla, N. V., Bowyer, K. W., Hall, L. O. & Kegelmeyer, W. P. SMOTE: Synthetic minority over-sampling technique. *J. Artif. Intell. Res.* **16**, 321–357 (2002).
- [59] Zhu, M. Recall, precision and average precision. *Department of Statistics and Actuarial Science, University of Waterloo, Waterloo* **2**, 6 (2004).
- [60] Sechidis, K., Tsoumakas, G. & Vlahavas, I. On the stratification of multi-label data. In *Machine Learning and Knowledge Discovery in Databases: European Conference, ECML PKDD 2011, Athens, Greece, September 5-9, 2011, Proceedings, Part III* **22**, 145–158 (Springer, 2011).
- [61] Morfi, V., Stowell, D. & Pamula, H. NIPS4Bplus: Transcriptions of NIPS4B 2013 Bird Challenge Training Dataset (2018). URL <https://doi.org/10.6084/m9.figshare.6798548>.
- [62] Morfi, V. & Stowell, D. Data-efficient weakly supervised learning for low-resource audio event detection using deep learning. In *Proceedings of the detection and classification of acoustic scenes and events 2018 workshop (DCASE)*, Proceedings of the detection and classification of acoustic scenes and events 2018 workshop, 123–127 (2018).
- [63] Bravo Sanchez, F. J., Hossain, M. R., English, N. B. & Moore, S. T. Bioacoustic classification of avian calls from raw sound waveforms with an open-source deep learning architecture. *Sci. Rep.* **11**, 15733 (2021).
- [64] Goller, F. & Riede, T. Integrative physiology of fundamental frequency control in birds. *J. Physiol. Paris* **107**, 230–242 (2013).
- [65] Lee, S., Lee, S. & Song, B. C. Improving vision transformers to learn small-size dataset from scratch. *IEEE Access* **10**,

- 123212–123224 (2022).
- [66] Howard, A., Klinck, H., Dane, S., Kahl, S. & Denton, T. Cornell birdcall identification (2020). URL <https://kaggle.com/competitions/birdsong-recognition>. Accessed: 2023-05-24.
- [67] Xeno-Canto Bird Recordings Extended (A-M). <https://www.kaggle.com/datasets/rohanrao/xeno-canto-bird-recordings-extended-a-m/versions/11>. Accessed: 2024-04-25.
- [68] Xeno-Canto Bird Recordings Extended (N-Z). <https://www.kaggle.com/datasets/rohanrao/xeno-canto-bird-recordings-extended-n-z/versions/11>. Accessed: 2024-04-25.
- [69] Longpre, S. *et al.* A pretrainer’s guide to training data: Measuring the effects of data age, domain coverage, quality, & toxicity. Preprint at <https://arxiv.org/abs/2305.13169> (2023).
- [70] Chen, H.-Y., Tu, C.-H., Li, Z.-H., Shen, H. & Chao, W.-L. On the importance and applicability of pre-training for federated learning. *Int Conf Learn Represent* (2022). 2206.11488.
- [71] Robinson, J. D. *et al.* Can contrastive learning avoid shortcut solutions? Conference on Neural Information Processing Systems (2021).
- [72] Tomasev, N. *et al.* Pushing the limits of self-supervised resnets: Can we outperform supervised learning without labels on imagenet? In *First Workshop on Pre-training: Perspectives, Pitfalls, and Paths Forward at ICML 2022* (2022).
- [73] Chen, T., Kornblith, S., Swersky, K., Norouzi, M. & Hinton, G. E. Big self-supervised models are strong semi-supervised learners. vol. 33, 22243–22255 (2020).
- [74] Baevski, A. *et al.* Data2vec: A general framework for self-supervised learning in speech, vision and language. In *International Conference on Machine Learning*, 1298–1312 (PMLR, 2022).
- [75] Saeed, A., Grangier, D. & Zeghidour, N. Contrastive learning of general-purpose audio representations. In *ICASSP 2021 - 2021 IEEE International Conference on Acoustics, Speech and Signal Processing (ICASSP)*, 3875–3879 (2021).
- [76] Brown, T. *et al.* Language models are few-shot learners. *Advances in neural information processing systems* **33**, 1877–1901 (2020).
- [77] Devlin, J., Chang, M.-W., Lee, K. & Toutanova, K. BERT: Pre-training of deep bidirectional transformers for language understanding. *NAACL HLT 2019 - 2019 Conference of the North American Chapter of the Association for Computational Linguistics: Human Language Technologies - Proceedings of the Conference* **1**, 4171–4186 (2018).
- [78] Liu, Y. *et al.* Roberta: A robustly optimized bert pretraining approach. Preprint at <https://arxiv.org/abs/1907.11692> (2019).
- [79] Hsu, W.-N. *et al.* HuBERT: Self-supervised speech representation learning by masked prediction of hidden units. *IEEE ACM Trans. Audio Speech Lang. Process.* **29**, 3451–3460 (2021).
- [80] Rethmeier, N. & Augenstein, I. A primer on contrastive pre-training in language processing: Methods, lessons learned, and perspectives. *ACM Computing Surveys* **55**, 1–17 (2023).
- [81] Lin, C.-C., Jaech, A., Li, X., Gormley, M. R. & Eisner, J. Limitations of autoregressive models and their alternatives. In Toutanova, K. *et al.* (eds.) *Proceedings of the 2021 Conference of the North American Chapter of the Association for Computational Linguistics: Human Language Technologies*, 5147–5173 (Association for Computational Linguistics, Online, 2021).
- [82] Zhu, D., Hedderich, M. A., Zhai, F., Adelani, D. & Klakow, D. Is bert robust to label noise? a study on learning with noisy labels in text classification. In *Proceedings of the Third Workshop on Insights from Negative Results in NLP*, 62–67 (2022).
- [83] Hinton, G., Vinyals, O. & Dean, J. Distilling the knowledge in a neural network. Preprint at <https://arxiv.org/abs/1503.02531> (2015).
- [84] Tarvainen, A. & Valpola, H. Mean teachers are better role models: Weight-averaged consistency targets improve semi-supervised deep learning results. *Advances in neural information processing systems* **30** (2017).
- [85] Grill, J.-B. *et al.* Bootstrap your own latent—a new approach to self-supervised learning. *Adv. Neural Inf. Process. Syst.* **33**, 21271–21284 (2020).
- [86] Caron, M. *et al.* Emerging properties in self-supervised vision transformers. In *Proceedings of the IEEE/CVF international conference on computer vision*, 9650–9660 (2021).
- [87] Baevski, A. *et al.* data2vec: A general framework for self-supervised learning in speech, vision and language. In Chaudhuri, K. *et al.* (eds.) *Proceedings of the 39th International Conference on Machine Learning*, vol. 162 of *Proceedings of Machine Learning Research*, 1298–1312 (PMLR, 2022).
- [88] Song, H., Kim, M., Park, D., Shin, Y. & Lee, J.-G. Learning from noisy labels with deep neural networks: A survey. *IEEE Trans. Neural Netw. Learn. Syst.* **34**, 8135–8153 (2023).
- [89] Oord, A. v. d., Li, Y. & Vinyals, O. Representation learning with contrastive predictive coding. Preprint at <https://arxiv.org/abs/1807.03748> (2018).
- [90] Chen, X., Fan, H., Girshick, R. & He, K. Improved baselines with momentum contrastive learning. Preprint at <https://arxiv.org/abs/2003.04297> (2020).
- [91] Lasseck, M. Audio-based bird species identification with deep convolutional neural networks. *CLEF (working notes)* **2125** (2018).
- [92] Li, L. *et al.* Automated classification of *Tursiops aduncus* whistles based on a depth-wise separable convolutional neural network and data augmentation. *J. Acoust. Soc. Am.* **150**, 3861 (2021).
- [93] Padovese, B., Frazao, F., Kirsebom, O. S. & Matwin, S. Data augmentation for the classification of north atlantic right whales upcalls. *J. Acoust. Soc. Am.* **149**, 2520 (2021).
- [94] Loshchilov, I. & Hutter, F. Decoupled weight decay regularization. In *International Conference on Learning Representations* (2018).
- [95] Srivastava, N., Hinton, G. E., Krizhevsky, A., Sutskever, I. & Salakhutdinov, R. Dropout: A simple way to prevent neural networks from overfitting. *J. Mach. Learn. Res.* **15**, 1929–1958 (2014).
- [96] Ba, J. L., Kiros, J. R. & Hinton, G. E. Layer normalization. Preprint at <https://arxiv.org/abs/1607.06450> (2016).
- [97] Tokozume, Y., Ushiku, Y. & Harada, T. Learning from between-class examples for deep sound recognition. In *International Conference on Learning Representations* (2018).
- [98] He, K., Zhang, X., Ren, S. & Sun, J. Delving deep into rectifiers:

- Surpassing human-level performance on imagenet classification. *Proceedings of the IEEE International Conference on Computer Vision* **11-18-Dece**, 1026–1034 (2016).
- [99] Ramachandran, P., Zoph, B. & Le, Q. V. Searching for activation functions. Preprint at <https://arxiv.org/abs/1710.05941> (2017).
- [100] Hendrycks, D. & Gimpel, K. Gaussian error linear units (GELUs). Preprint at <https://arxiv.org/abs/1606.08415> (2016).
- [101] He, K. *et al.* Masked autoencoders are scalable vision learners. In *Proceedings of the IEEE/CVF Conference on Computer Vision and Pattern Recognition (2022)*, 16000–16009 (2022).
- [102] Loshchilov, I. & Hutter, F. SGDR: Stochastic gradient descent with warm restarts. *International Conference on Learning Representations* (2017).
- [103] Bengio, Y., Frasconi, P. & Simard, P. The problem of learning long-term dependencies in recurrent networks. In *IEEE International Conference on Neural Networks*, 1183–1188 vol.3 (IEEE, 2002).
- [104] Paszke, A. *et al.* PyTorch: An imperative style, high-performance deep learning library. *Advances in neural information processing systems* **32** (2019).
- [105] Ott, M. *et al.* fairseq: A fast, extensible toolkit for sequence modeling. In *Proceedings of NAACL-HLT 2019: Demonstrations* (2019).
- [106] Federal Statistical Office of Germany (Statistisches Bundesamt - Destatis). Electricity consumption of households by household size. <https://www.destatis.de/EN/Themes/Society-Environment/Environment/Environmental-Economic-Accounting/private-households/Tables/electricity-consumption-private-households.html>. Accessed: 2024-05-06.
- [107] Electricity Maps ApS. Yearly averaged emission factor for 2023. <https://app.electricitymaps.com/zone/DE>. Accessed: 2023-05-24.
- [108] Jouppi, Norm and Patterson, David. Google’s Cloud TPU v4 provides exaFLOPS-scale ML with industry-leading efficiency. <https://shorturl.at/jlmW4>. Accessed: 2024-05-08.
- [109] Lin, T.-Y., Goyal, P., Girshick, R., He, K. & Dollár, P. Focal loss for dense object detection. In *2017 IEEE International Conference on Computer Vision (ICCV)*, 2999–3007 (2017).
- [110] Meyses, R., Lu, M., de Puiseau, C. W. & Meisen, T. Ablation studies in artificial neural networks. Preprint at <https://arxiv.org/abs/1901.08644> (2019).
- [111] Gwilliams, L., King, J., Marantz, A. & Poeppel, D. Neural dynamics of phoneme sequences reveal position-invariant code for content and order. *Nat. Commun.* **13** (2022).
- [112] Ma, G., Hu, P., Kang, J., Huang, S. & Huang, H. Leveraging phone mask training for phonetic-reduction-robust e2e uyghur speech recognition. Preprint at <https://arxiv.org/abs/2204.00819> (2022).
- [113] Boyd, K., Eng, K. H. & Page, C. D. Area under the precision-recall curve: Point estimates and confidence intervals. In *Advanced Information Systems Engineering*, Lecture notes in computer science, 451–466 (Springer Berlin Heidelberg, Berlin, Heidelberg, 2013).
- [114] Bahdanau, D., Cho, K. & Bengio, Y. Neural machine translation by jointly learning to align and translate. Preprint at <https://arxiv.org/abs/1409.0473> (2014).
- [115] Luong, M.-T., Pham, H. & Manning, C. D. Effective approaches to attention-based neural machine translation. In *Proceedings of the 2015 Conference on Empirical Methods in Natural Language Processing*, 1412–1421 (2015).
- [116] Jain, S. & Wallace, B. C. Attention is not explanation. In *Proceedings of the 2019 Conference of the North American Chapter of the Association for Computational Linguistics: Human Language Technologies, Volume 1 (Long and Short Papers)*, 3543–3556 (2019).
- [117] Wiegreffe, S. & Pinter, Y. Attention is not not explanation. In *Proceedings of the 2019 Conference on Empirical Methods in Natural Language Processing and the 9th International Joint Conference on Natural Language Processing (EMNLP-IJCNLP)*, 11–20 (2019).
- [118] Akula, A. R. & Zhu, S.-C. Attention cannot be an explanation. Preprint at <https://arxiv.org/abs/2201.11194> (2022).
- [119] Bibal, A. *et al.* Is attention explanation? an introduction to the debate. In Muresan, S., Nakov, P. & Villavicencio, A. (eds.) *Proceedings of the 60th Annual Meeting of the Association for Computational Linguistics (Volume 1: Long Papers)*, 3889–3900 (Association for Computational Linguistics, Stroudsburg, PA, USA, 2022).
- [120] Yeh, C. *et al.* AttentionViz: A global view of transformer attention. *IEEE Trans. Vis. Comput. Graph.* **30**, 262–272 (2024). 2305.03210.
- [121] Engesser, S. & Manser, M. B. Collective close calling mediates group cohesion in foraging meerkats via spatially determined differences in call rates. *Anim. Behav.* **185**, 73–82 (2022).
- [122] Demartsev, V. *et al.* Mapping vocal interactions in space and time differentiates signal broadcast versus signal exchange in meerkat groups. *Philos. Trans. R. Soc. Lond. B Biol. Sci.* **379** (2024).
- [123] Fan, A., Grave, E. & Joulin, A. Reducing transformer depth on demand with structured dropout. In *International Conference on Learning Representations* (2019).

Data availability

The MeerKAT dataset is openly available at the Max-Planck data repository Edmond [43] under a CC BY-NC license [42].

Code availability

The code for animal2vec and the weights for our pretrained and finetuned transformer models are available at our GitHub [41] under an MIT license [40].

Acknowledgments

We thank Rebecca Schäfer for their immense help during the field data collection. We are indebted to many student research assistants for their help with processing and labeling of the audio data (L. Leonardos, C. Maier, J. Denger, L. Batke, S. Eleonori, F. Raabe, H. Brønnevik, J. Ruff, B. Ehrmann and S. Knab). We are grateful to the Kalahari Research Trust and Northern Cape Department of Environment and Nature

Conversation for research permission at the Kalahari Research Centre, as well as the support of the Universities of Cambridge and Zurich, and MAVA foundation on the maintenance of the habituated meerkat population. We thank T. Vink and W. Jubber for organizing the field site, the managers and volunteers of the Kalahari Meerkat Project for maintaining habituation and long-term data collection of the meerkats.

This research was supported by

Max Planck Society; Alexander von Humboldt-Stiftung; Centre for the Advanced Study of Collective Behaviour: EXC 2117-422037984; Human Frontier Science Program: RGP0051/2019; Minerva Foundation; Gips-Schüle Foundation; Young Scholars Fund at the University of Konstanz; Alexander von Humboldt Foundation post-doctoral fellowships; The long-term research on meerkats is currently supported by funding from the European Research Council (ERC) under the European Union's Horizon 2020 research and innovation program (No. 742808 and No. 294494) and a Grant from the Natural Environment Research Council (Grant NE/G006822/1) to Tim Clutton-Brock, as well as by Grants from the University of Zurich to M.B.M. and the MAVA Foundation.

Ethics

All procedures were approved by ethical committees of University of Pretoria, South Africa (permit: EC031-17) and the Northern Cape Department of Environment and Nature Conservation (permit: FAUNA 1020/2016).

Authors' contributions

The field studies at the KRC in 2017 and 2019 were performed by V.D., B.A., G.G., L.J.U., M.B.M., and A.S.P.. Data labeling was performed by many student research assistants (see Acknowledgments) under the supervision of V.D., B.A., and A.S.P.. Data cleaning and post-processing were performed by V.D. and J.C.S.Z.. Early studies using different deep learning architectures in combination with the MeerKAT dataset were performed by K.D.A., M.D., and D.S.. The conceptual idea for animal2vec was conceived by J.C.S.Z., where M.A.R., A.S.P., and J.C.S.Z. jointly analyzed the results of animal2vec. J.C.S.Z. wrote the codebase for animal2vec, with guidance from M.A.R., where M.F. and M.A.R. conducted a code review before publication. The figures were created by J.C.S.Z.. The initial manuscript draft was written by J.C.S.Z.. All authors provided edits and feedback on the final manuscript.

Conflict of Interest

The authors declare no competing financial or non-financial interests.

Appendix

TABLE V. Training parameter for pretraining the animal2vec framework on MeerKAT and xeno canto.

Parameter	Pretraining setting		
	MeerKAT	Xeno canto	Transformer baseline [38]
Learning rate	1×10^{-4}	2.5×10^{-4}	1×10^{-4}
Adam β_1 / β_2	0.9 / 0.98	0.9 / 0.98	0.9 / 0.98
Weight decay	0.01	0.01	0.01
Clip norm	1	1	1
Learning rate schedule	cosine	cosine	cosine
Warmup steps	10 000	8000	10 000
GPUs	4 A100-SXM4-80GB	4 3090Ti-24GB	4 A100-SXM4-80GB
Batch size (sec. p. GPU / total)	255 / 1020	250 / 1000	255 / 1020
Transformer layers	16	12	16
Attention heads	16	12	16
Embedding dimensions	1024	768	1024
Updates	408 000 (100 epochs)	264 600 (100 epochs)	408 000 (100 epochs)
Decoder dim.	768	384	768
Decoder conv. groups	16	16	16
Decoder kernel width	7	7	7
Decoder layers	4	4	4
Mask probability p	0.1500	0.1500	0.0650
Mask length M	2	2	10
Nr. of Sinc filters [37]	127	127	-
Sinc filter kernel width [37]	63	125	-
BCL mixing strength (target) [97]	0	0	0
BCL mixing strength (input) [97]	0.5	0.5	0
BCL token prob. [97]	1.0	1.0	0
BCL window length [97]	0.05	0.05	0
PSwish initial α	2	2	-
PSwish initial β	0	0	-
	(512, 10, 5)	(512, 10, 5)	(512, 10, 5)
	(512, 3, 2)	(512, 3, 2)	(512, 3, 2)
	(512, 3, 2)	(512, 3, 2)	(512, 3, 2)
Feature Extractor layout	(512, 3, 2)	(512, 3, 2)	(512, 3, 2)
(Nr. of filter, width, stride)	(512, 3, 1)	(512, 3, 2)	(512, 3, 2)
	(512, 2, 1)	(512, 2, 1)	(512, 2, 2)
	(512, 2, 1)	(512, 2, 1)	(512, 2, 2)
Nr. of trainable parameters	315M	94M	315M

TABLE VI. Training parameter for finetuning the animal2vec framework on MeerKAT and NIPS4Bplus.

Parameter	Finetune setting				
	MeerKAT (1 %)	MeerKAT (25 %)	MeerKAT (100 %)	Baseline (100 %)	NIPS4Bplus
Learning rate	1×10^{-4}	7.5×10^{-5}	3×10^{-5}	3×10^{-5}	1×10^{-4}
Adam β_1 / β_2	0.9 / 0.98	0.9 / 0.98	0.9 / 0.98	0.9 / 0.98	0.9 / 0.98
Learning rate schedule	cosine	cosine	cosine	cosine	cosine
GPUs		4 A100-SXM4-80GB			4 3090Ti-24GB
Batch size (sec. p. GPU / total)	480 / 1920	480 / 1920	480 / 1920	480 / 1920	392 / 1568
Warmup steps	2000	2000	2000	2000	1000
Steps with fixed transformer	10 000	10 000	10 000	10 000	3000
Steps with transformer	3000 (1000 epochs)	8000 (107 epochs)	20 000 (67 epochs)	20 000 (67 epochs)	2000 (913 epochs)
Total steps	13 000 (4333 epochs)	18 000 (240 epochs)	30 000 (100 epochs)	30 000 (100 epochs)	5000 (2283 epochs)
Mask probability p	0.1100	0.1000	0.0825	0.0650	0.1100
Mask length M	2	3	4	10	2
BCL mixing strength (target) [97]	0.5	0.5	0.5	0	0.5
BCL mixing strength (input) [97]	0.5	0.5	0.5	0	0.5
BCL token prob. [97]	1.0	1.0	1.0	0	1.0
BCL window length [97]	0.05	0.05	0.05	0	0.05
γ in Focal loss [109]	2	2	2	0	2
Averaging over K transformer layers	16	16	16	8	12
Dropout [95]	0.1	0.1	0.1	0.1	0.1
Layerdrop [123]	0.1	0.1	0.1	0.1	0.1

Globally averaged attention map

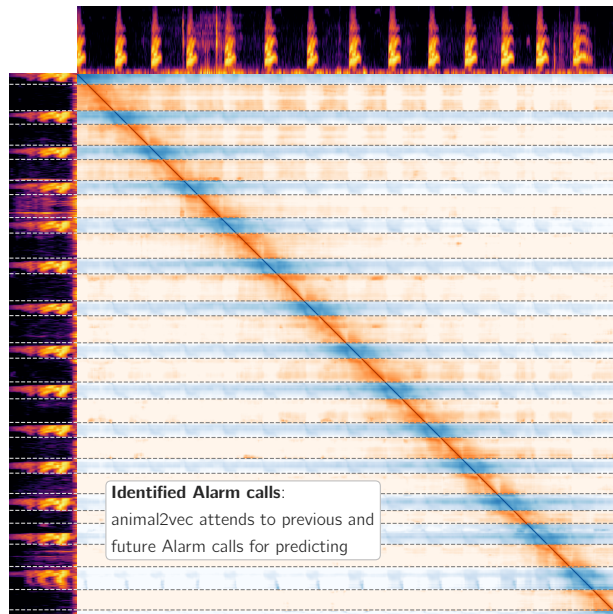


FIG. 7. Globally averaged attention map of a four second segment showing four move calls. An attention map shows the *importance* of every input frame with respect to every other frame during finetuning. Blue stretches surrounded by dashed white lines correspond to the predictions of animal2vec. For predicting, animal2vec attends to the immediate past and future of an event, as well as to previous and future alarm calls.

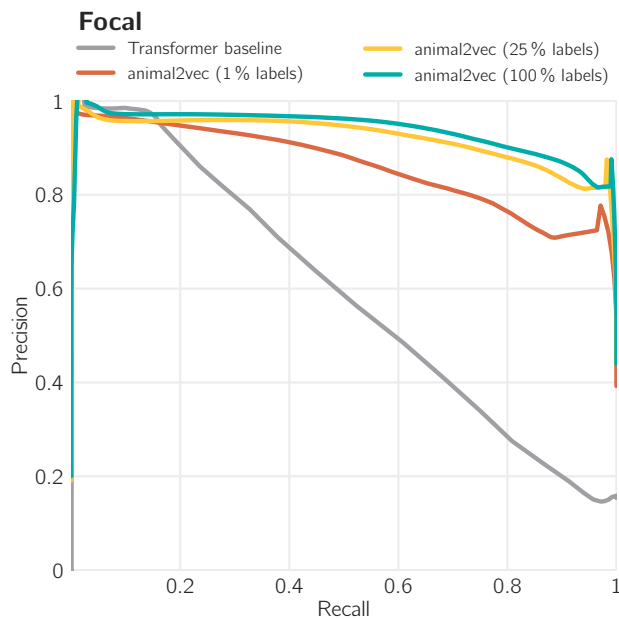


FIG. 8. The precision-recall curve for the focal class. Results of animal2vec using 1%, 25%, and 100% of the training data are in red, yellow, and teal, respectively, and the baseline results are in gray.

Close call

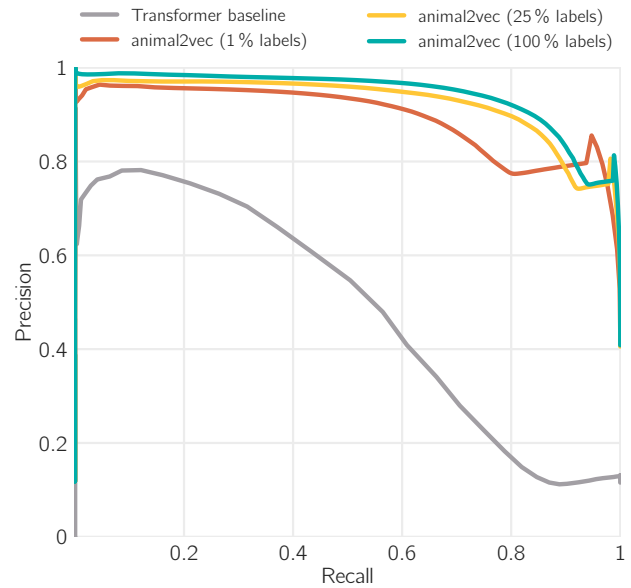


FIG. 9. The precision-recall curve for the close call class. Results of animal2vec using 1%, 25%, and 100% of the training data are in red, yellow, and teal, respectively, and the baseline results are in gray.

Short-note call

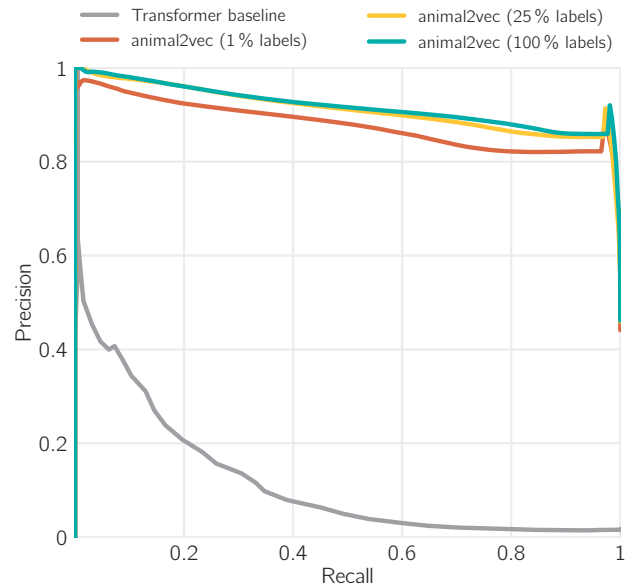


FIG. 10. The precision-recall curve for the short-note call class. Results of animal2vec using 1%, 25%, and 100% of the training data are in red, yellow, and teal, respectively, and the baseline results are in gray.

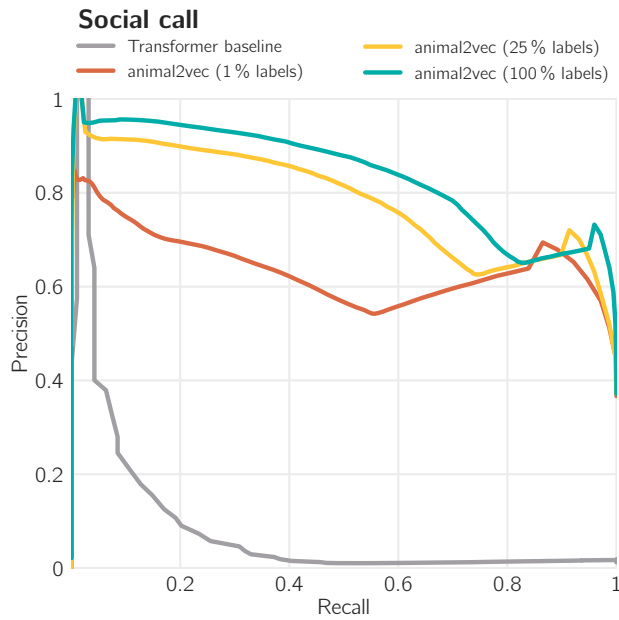


FIG. 11. The precision-recall curve for the social call class. Results of animal2vec using 1%, 25%, and 100% of the training data are in red, yellow, and teal, respectively, and the baseline results are in gray.

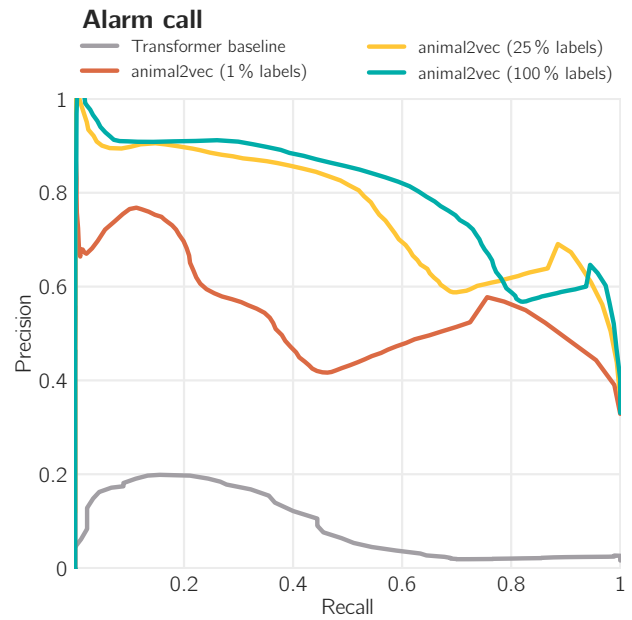


FIG. 13. The precision-recall curve for the alarm call class. Results of animal2vec using 1%, 25%, and 100% of the training data are in red, yellow, and teal, respectively, and the baseline results are in gray.

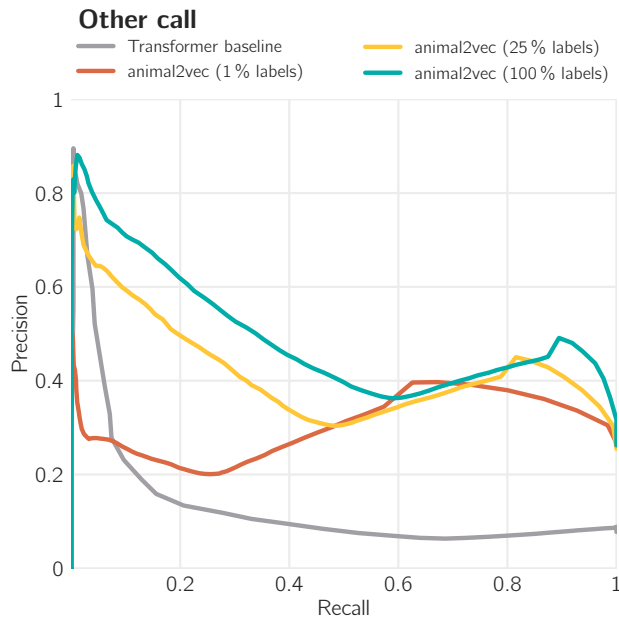


FIG. 12. The precision-recall curve for the other call class. Results of animal2vec using 1%, 25%, and 100% of the training data are in red, yellow, and teal, respectively, and the baseline results are in gray.

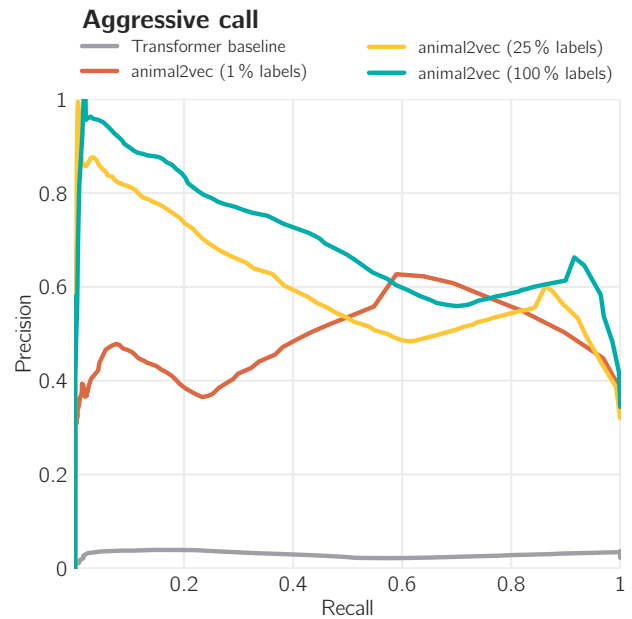


FIG. 14. The precision-recall curve for the aggressive call class. Results of animal2vec using 1%, 25%, and 100% of the training data are in red, yellow, and teal, respectively, and the baseline results are in gray.

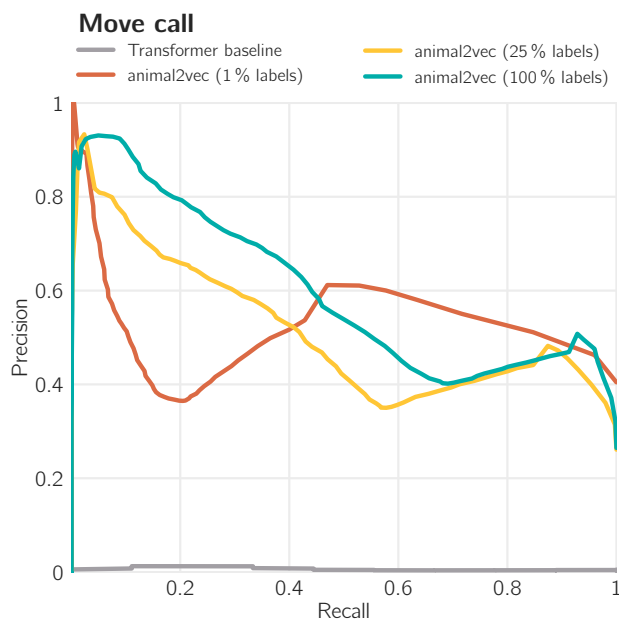


FIG. 15. The precision-recall curve for the move call class. Results of animal2vec using 1%, 25%, and 100% of the training data are in red, yellow, and teal, respectively, and the baseline results are in gray.

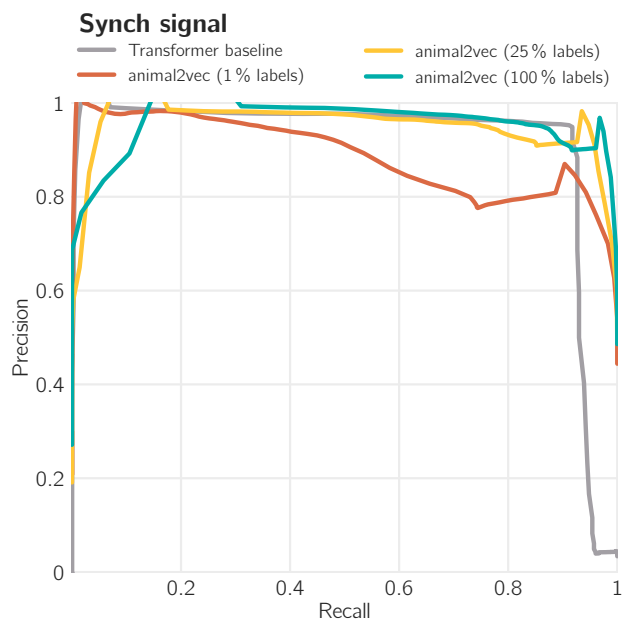


FIG. 17. The precision-recall curve for the synch signal class. Results of animal2vec using 1%, 25%, and 100% of the training data are in red, yellow, and teal, respectively, and the baseline results are in gray.

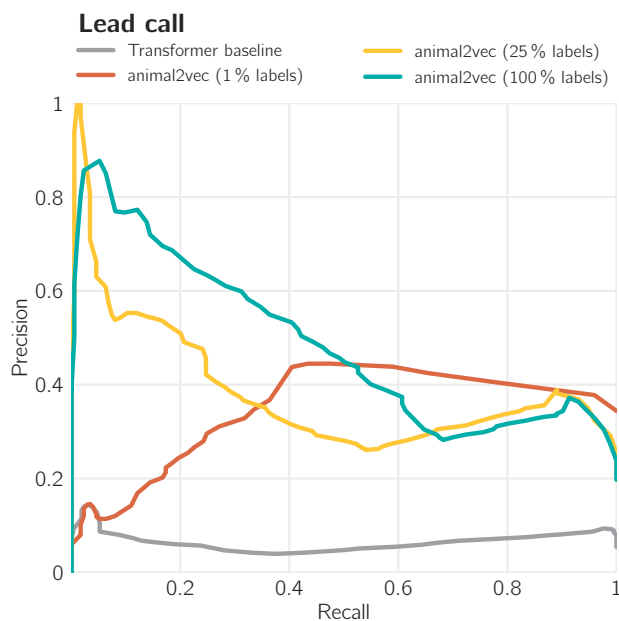


FIG. 16. The precision-recall curve for the lead call class. Results of animal2vec using 1%, 25%, and 100% of the training data are in red, yellow, and teal, respectively, and the baseline results are in gray.

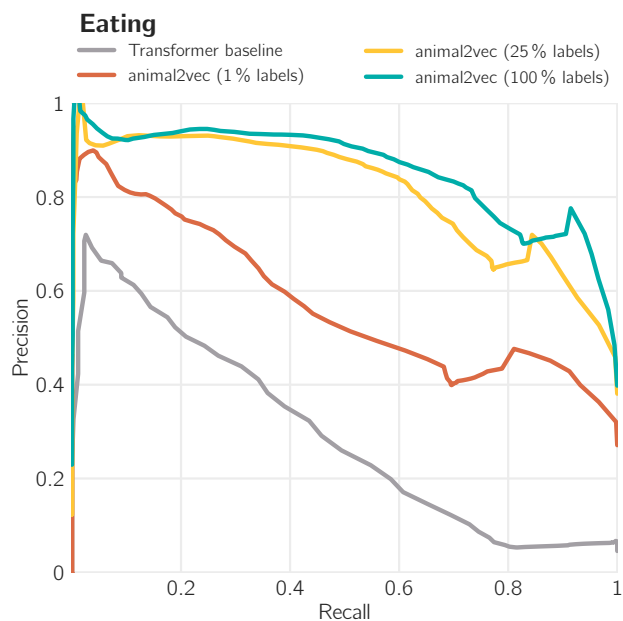


FIG. 18. The precision-recall curve for the eating class. Results of animal2vec using 1%, 25%, and 100% of the training data are in red, yellow, and teal, respectively, and the baseline results are in gray.

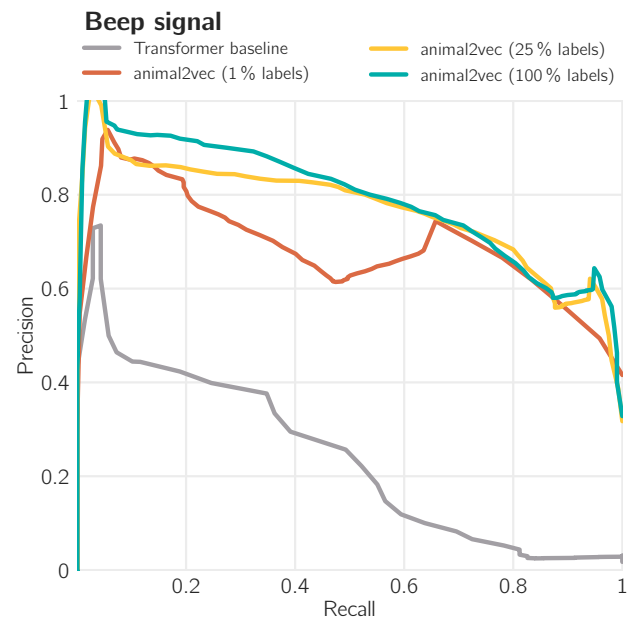


FIG. 19. The precision-recall curve for the beep signal class. Results of animal2vec using 1%, 25%, and 100% of the training data are in red, yellow, and teal, respectively, and the baseline results are in gray.